

# Repeater-Like Asynchronous Measurement-Device-Independent Quantum Conference Key Agreement

Yu-Shuo Lu,<sup>1,2,\*</sup> Yuan-Mei Xie,<sup>1,2,\*</sup> Yao Fu,<sup>3</sup> Hua-Lei Yin,<sup>2,1,4,†</sup> and Zeng-Bing Chen<sup>1,‡</sup>

<sup>1</sup>*National Laboratory of Solid State Microstructures and School of Physics,  
Collaborative Innovation Center of Advanced Microstructures, Nanjing University, Nanjing 210093, China*

<sup>2</sup>*Department of Physics and Beijing Key Laboratory of Opto-electronic Functional Materials and Micro-nano Devices,  
Key Laboratory of Quantum State Construction and Manipulation (Ministry of Education),  
Renmin University of China, Beijing 100872, China*

<sup>3</sup>*Beijing National Laboratory for Condensed Matter Physics and Institute of Physics,  
Chinese Academy of Sciences, Beijing 100190, China*

<sup>4</sup>*Beijing Academy of Quantum Information Sciences, Beijing 100193, China*

(Dated: June 25, 2024)

Quantum conference key agreement facilitates secure communication among multiple parties through multipartite entanglement and is anticipated to be an important cryptographic primitive for future quantum networks. However, the experimental complexity and low efficiency associated with the synchronous detection of multipartite entangled states have significantly hindered their practical application. In this work, we propose a measurement-device-independent conference key agreement protocol that utilizes asynchronous Greenberger-Horne-Zeilinger state measurement. This approach achieves a linear scaling of the conference key rate among multiple parties, exhibiting performance similar to that of the single-repeater scheme in quantum networks. The asynchronous measurement strategy bypasses the need for complex global phase locking technologies, concurrently extending the intercity transmission distance with composable security in the finite key regime. Additionally, our work also showcases the advantages of the asynchronous pairing concept in multiparty quantum entanglement.

*Introduction.*— Quantum networks revolutionize various communication tasks among multiple parties through quantum physics [1–4]. Quantum conference key agreement (QCKA) enables a group of users in a quantum network to efficiently distribute information-theoretically secure conference keys [5–7] with potential applications ranging from net meetings to financial transactions and telemedicine. The foundation of QCKA lies in establishing multipartite entanglement [8] among distant participants. Intuitively, this can be achieved by directly distributing the Greenberger-Horne Zeilinger (GHZ) state [9]. This approach has been extensively studied in various scenarios [10–21]. However, the practical application of this approach is hindered by the complexity of preparing and distributing high-fidelity entangled states in real quantum networks. More seriously, recent theories [22, 23] have shown that there is a performance limit for distributing multipartite entanglement in repeaterless quantum networks, thereby establishing an upper bound on the rates at which conference keys can be generated. Specifically, the single-message multicast bound in a star network is given by  $R \leq -\log_2(1 - \eta_i)$  [23], where  $\eta_i$  is the channel transmittance between two users in the quantum network, indicating that the rate of the conferencing key cannot surpass the Pirandola-Laurenza-Ottaviani-Banchi (PLOB) bound [24].

To break the PLOB bound, twin-field quantum key distribution [25] and asynchronous measurement-device-independent (AMDI) quantum key distribution [26] (also referred to as mode-pairing quantum key distribution [27]) are the feasible ways that can be implemented with current technology. The most critical element is the introduction of an untrusted relay node architecture, first proposed in MDI quantum key distribution [28]. This architecture resembles a single-node quantum repeater but does not require quantum memory. By utilizing the untrusted relay node architecture, one can resist all detector attacks and avoid the need for actively preparing and distributing entangled states. Unfortunately, while MDI-QCKA [6, 29] and phase-matching QCKA [30] follow this architecture, they achieve much lower rates than PLOB bound. Specifically, their key rates decrease exponentially with the number of participants. In addition, some efforts [31–33] have been made to break PLOB bound beyond current technical conditions, such as a complex beam splitter network that changes as the participant changes [33].

TABLE I. Summary of the key features of recent QCKA protocols.

	Removing phase locking	Breaking the bound	Finite key	General $N$ party
This work	Yes	Yes	Yes	Yes
Fu <i>et al.</i> [6]	Yes	-	-	Yes
Zhao <i>et al.</i> [30]	-	-	-	Yes
Li <i>et al.</i> [15]	-	-	-	-
Carrara <i>et al.</i> [33]	-	Yes	-	Yes

\* These authors contributed equally.

† hlyin@ruc.edu.cn

‡ zbchen@nju.edu.cn

In this work, inspired by AMDI quantum key distribution [26, 27] and the post-matching method [34], we propose an AMDI-QCKA protocol that utilizes the asynchronous multi-photon interference in the untrusted relay node architecture. The implementation of asynchronous multi-photon interference involves a  $2N$ -shaped cyclic multi-interference network with  $N$  detection ports. By pairing  $N$  interference events at different ports with temporal separation within the coherent time  $T_c$ , effective GHZ-measurement events can be obtained. The key rate scales as  $O(\eta)$  in the high count rate limit, where there are sufficient click events within the coherent time. Here,  $\eta$  denotes the channel transmittance between the user and the untrusted relay. Therefore, our protocol can break the PLOB bound and achieve a transmission distance of over 400 km. By employing phase-randomized weak coherent sources and the decoy state method [35, 36], we also provide a solution for obtaining a secure conference key rate in finite size with composable security. Additionally, the asynchronous pair strategy has been proven to eliminate the need for complex global phase locking techniques [37, 38]. A comparison of recent QCKA protocols is shown in Tab. I.

*Protocol.*— The topology of the  $N$ -user AMDI-QCKA network is shown in Fig. 1. There are  $N$  users labeled  $U_1, U_2, \dots, U_N$ , and an untrusted intermediate measurement node controlled by Eve. Each user is equipped with a laser, an intensity modulator, a phase modulator and an attenuator, all employed to generate phase-randomized weak coherent pulses at single-photon level. Controlled by Eve, the measurement node can be any structure, with the expectation of having  $N$  detection ports  $P_1, P_2, \dots, P_N$  forming a  $2N$ -sided shape. Each port  $P_i$  ( $i \in \{1, 2, \dots, N\}$ ) contains a 50/50  $2 \times 2$  beam splitter (BS) and two single photon detectors,  $L_i$  and  $R_i$ . The AMDI-QCKA protocol for  $N$  users is given as follows.

**Step 1 (Preparation):** For each time bin, each user  $U_i$  prepares a phase-randomized weak coherent pulse  $|e^{i\theta_i} \sqrt{k_i}\rangle$  with intensity  $k_i$ , probability  $p_{k_i}$ , random phase  $\theta_i = 2\pi M_i/M$ , random intensity  $k_i \in \{\mu_i, \nu_i, o\}$  (signal, decoy, and vacuum state,  $\mu_i > \nu_i > o$ ), where  $M_i \in \{0, 2, \dots, M-1\}$  represents the random phase slice. All the users send their pulses to Eve.

**Step 2 (Measurement):** Eve performs interference measurement on the received pulses, with each user's pulse interfering with those of its two neighboring users. The pulse from each user is first split by a  $1 \times 2$  BS, and then directed to two neighbor ports. At detection port  $P_i$  ( $i \neq N$ ), the pulses from  $U_i$  interfere with those from  $U_{i+1}$ , and at  $P_N$ , the pulses from  $U_N$  interfere with those from  $U_1$ . In each time bin, successful click events are recorded only when a single detector click occurs. Eve publishes all successful click events and the corresponding detectors.

**Step 3 (Pairing):** The users pair  $N$  successful click events occurring in  $N$  different detection ports with a time interval less than the maximum pairing time  $T_c$  to obtain a pairing event. At the time bin when  $P_i$  ( $i \neq N$ ) obtains

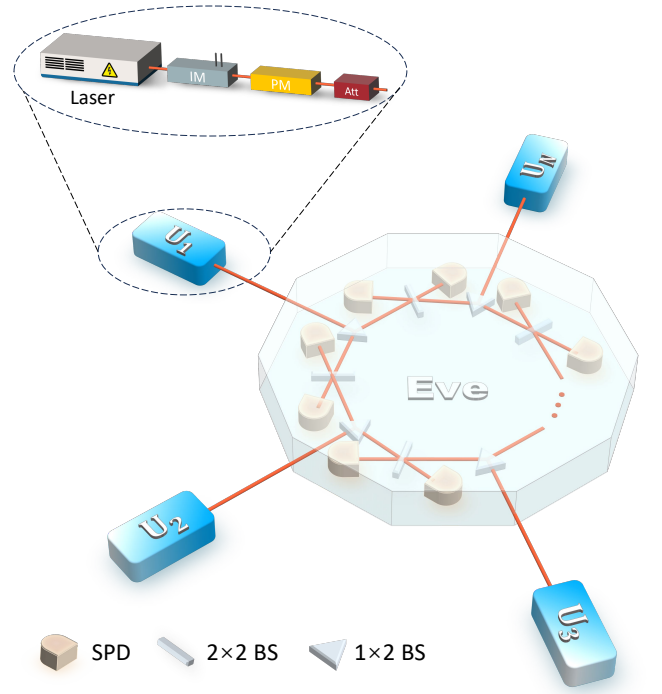


FIG. 1. Conceptual schematic of the AMDI-QCKA protocol. There are  $N$  users connected to an untrusted measurement node, Eve, via optical channels. Each user employs a laser, intensity modulator (IM), phase modulator (PM) and attenuator (Att) to prepare phase-randomized weak coherent pulses. Eve is expected to be composed of  $N$  detection ports, which collectively form a  $2N$ -sided shape. Each detection port includes a  $2 \times 2$  beam splitter (BS) and two single-photon detectors (SPD) connecting the left and right output of BS. The optical pulses from each user are split by the  $1 \times 2$  BS into two parts, which are directed to two neighboring measurement ports, and interfere with that from the neighboring users.

a single click,  $U_i$  ( $U_{i+1}$ ) registers a late (early) time bin, represented with superscript  $l(e)$ . When  $P_N$  clicks,  $U_N$  ( $U_1$ ) registers a late (early) time bin. Each user  $U_i$  calculates  $k_i^{\text{tot}} = k_i^e + k_i^l$ , representing the total intensity used in two time bins where  $U_i$ 's two neighboring detection ports have single clicks and the global phase difference  $\theta_i = \theta_i^l - \theta_i^e$ .

**Step 4 (Sifting):** For each pairing event, each user  $U_i$  publicly announces  $k_i^{\text{tot}}$  and  $\theta_i$ . The paired event can be represented as  $[k_1^{\text{tot}}, k_2^{\text{tot}}, \dots, k_N^{\text{tot}}]$ . The participants assign  $[\mu_1, \mu_2, \dots, \mu_N]$  events to  $\mathbf{Z}$ -basis. For pairing event  $[2\nu_1, 2\nu_2, \dots, 2\nu_N]$ , they calculate the sum of the global phase difference  $\theta_g = \sum_{i=1}^N \theta_i$ . If  $\theta_g/\pi \bmod 2 = 0$  or  $1$ , they assign it to  $\mathbf{X}$ -basis. The number of other pairing events is used in parameter estimation. For a pairing event in the  $\mathbf{Z}$ -basis, each user  $U_i$  obtains a bit value 0 if  $k_i^e = \mu_i$  and  $k_i^l = o$ . Otherwise, an opposite bit is extracted. In the  $\mathbf{X}$ -basis, they obtain bit values according to the click detector and the value of  $\theta_g/\pi \bmod 2$ . The key mapping rule in the  $\mathbf{X}$ -basis is shown in Table II.

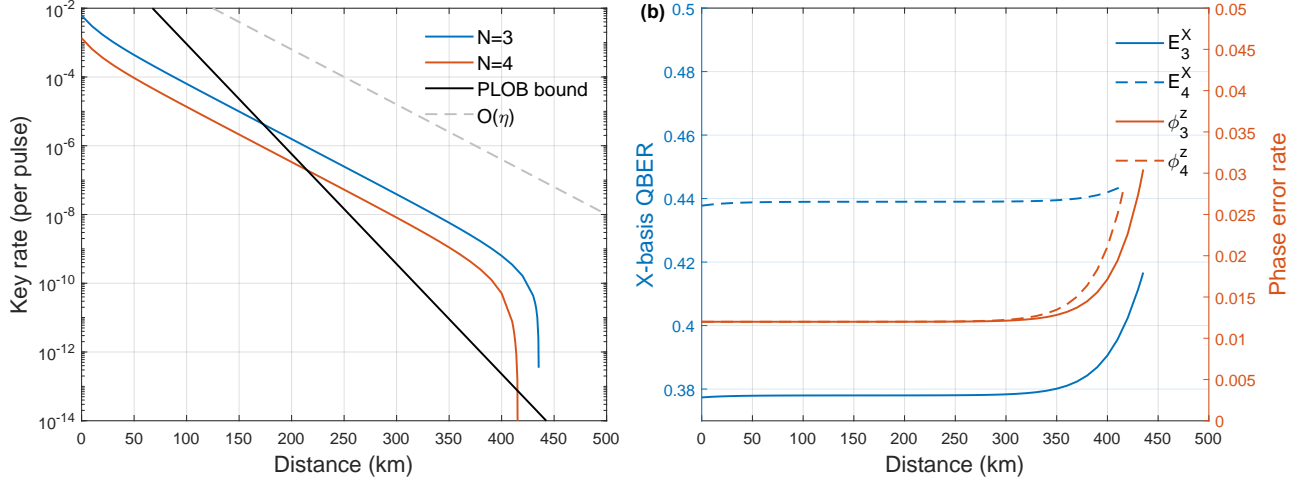


FIG. 2. Simulation results of the conference key rate and the error rate are presented as functions of the transmission distance between users and Eve. The three-user and four-user cases in the asymptotic limit with an infinite number of decoy states in symmetric channels are considered. For all simulations, we employ the same parameters: fiber channel loss coefficient  $0.16 \text{ dB km}^{-1}$ , detection efficiency 85%, dark counting rate  $10^{-10}$ , error correction efficiency  $f=1.02$  and  $\mathbf{X}$ -basis misalignment  $e_d = 1.2\%$ . Here, we assume the global phase locking is utilized. (a) Conference key rate as a function of distance. (b) The  $\mathbf{Z}$ -basis phase error rate  $\phi_N^z$  and the  $\mathbf{X}$ -basis quantum bit error rate (QBER) as functions of distance.

Step 6 (Parameter estimation and postprocessing): By using the decoy state method, in the  $\mathbf{Z}$ -basis, they estimate the probability of obtain a joint  $N$ -photon events  $\tilde{Y}_N^z$  per pulse and the phase error rate  $\phi_N^z$ . By using multiparty entanglement-distillation techniques [6, 9], the final key rate can be given as

$$R = \tilde{Y}_N^z [1 - H_2(\phi_N^z)] - \text{leak}_{\text{EC}}, \quad (1)$$

where  $\text{leak}_{\text{EC}} = \max_{2 \leq i \leq N} [H_2(E_{1,i}^z)] f \tilde{Q}_{[\mu_1, \mu_2, \dots, \mu_N]}^z$  is the amount of information leaked during multy-party error correction,  $\tilde{Q}_{[\mu_1, \mu_2, \dots, \mu_N]}^z$  is the probability of obtaining a  $[\mu_1, \mu_2, \dots, \mu_N]$  event per pulse,  $H_2(x) = -x \log_2 x - (1-x) \log_2 (1-x)$  is the binary Shannon entropy function, and  $f$  is the error correction efficiency. We consider the key of the  $U_1$  as the reference key,  $E_{1,i}^z$  is the marginal bit error rate between  $U_1$  and  $U_i$ .

Specifically, the key length formula in finite size regime against coherent attack with  $\varepsilon_{\text{cor}}$ -correctness and  $\varepsilon_{\text{sec}}$  secrecy when  $N = 3$  can be written as

$$l \geq \underline{s}_0^z + \underline{s}_3^z (1 - H_2(\bar{\phi}_3^z)) - \text{leak}_{\text{EC}} - \log_2 \frac{4}{\varepsilon_{\text{cor}}} - 2 \log_2 \frac{2}{\varepsilon' \hat{\varepsilon}} - 2 \log_2 \frac{1}{2\varepsilon_{\text{PA}}}, \quad (2)$$

TABLE II. The key mapping rule in the  $\mathbf{X}$ -basis.  $r_i = 0$  (1) represents the detector  $L_i$  ( $R_i$ ) clicks.

$(\theta_g)/\pi$ mod 2	$U_1$ 's bit	$U_i$ 's bit ( $i \in \{2, \dots, N\}$ )
0	$[\theta_1/\pi \text{ mod } 2] \oplus r_1 \oplus \dots \oplus r_N \oplus 0$	$[\theta_i/\pi \text{ mod } 2]$
1	$[\theta_1/\pi \text{ mod } 2] \oplus r_1 \oplus \dots \oplus r_N \oplus 1$	$[\theta_i/\pi \text{ mod } 2]$
Others	Discard	

where  $\underline{x}$  and  $\bar{x}$  are the lower and upper bounds of the observed value  $x$ , respectively,  $\underline{s}_0^z$ ,  $\underline{s}_3^z$ , and  $\bar{\phi}_3^z$  are the number of  $[0, \mu_1, \mu_2]$  events, the number of joint three-photon component of  $[\mu_1, \mu_2, \mu_3]$  events and the corresponding phase error rate, respectively, where  $\text{leak}_{\text{EC}} = \max_{2 \leq i \leq 3} [H_2(E_{1,i}^z)] f n_{[\mu_1, \mu_2, \mu_3]}^z$  is the amount of information leaked during multy-party error correction,  $n_{[\mu_1, \mu_2, \mu_3]}^z$  is the number of  $[\mu_1, \mu_2, \mu_3]$  event. The overall security  $\varepsilon_{\text{tot}}$  is defined as:  $\varepsilon_{\text{tot}} = \varepsilon_{\text{sec}} + \varepsilon_{\text{cor}}$ ,  $\varepsilon_{\text{sec}} = 2(\varepsilon' + 2\varepsilon_e + \hat{\varepsilon}) + \varepsilon_0 + \varepsilon_3 + \varepsilon_\beta + \varepsilon_{\text{PA}}$ , where  $\varepsilon'$ ,  $\varepsilon_e$ ,  $\hat{\varepsilon}$  and  $\varepsilon_e$  are security parameters,  $\varepsilon_0$ ,  $\varepsilon_3$  and  $\varepsilon_\beta$  quantify the failure probabilities in estimating the terms of  $\underline{s}_0^z$ ,  $\underline{s}_3^z$ , and  $\bar{\phi}_3^z$ , respectively. Detailed formulas for decoy-state estimation are shown in the Supplemental Material.

*Performance.*— We numerically simulate the conference key rate of the AMDI-QCKA protocol in symmetric channels. The light intensities and the corresponding probabilities are globally optimized. To demonstrate the performance in the ideal case, we first consider users may choose infinite number of decoy states in asymptotic regime and assume that global phase locking is employed. The use of phase locking indicates that the coherent time between user are infinite, resulting in infinite  $T_c$ . Therefore, all detection events are paired. As shown in Fig. 2(a), in both the  $N = 3$  and  $N = 4$  cases, our protocol can overcome the PLOB bound and shows a linear scaling of key rate as  $\eta$  up to 400 km. The phase error rate and the  $\mathbf{X}$ -basis quantum bit error rate (QBER) are shown in Fig. 2(b). There exists an intrinsic  $\mathbf{X}$ -basis QBER of about 37.5% for  $N = 3$  and 43% for  $N = 4$ , respectively, attributed to the multi-photon components in the coherent state. In a paired event, the pulses transmitted by user  $U_i$  in two time bins constitute a part of

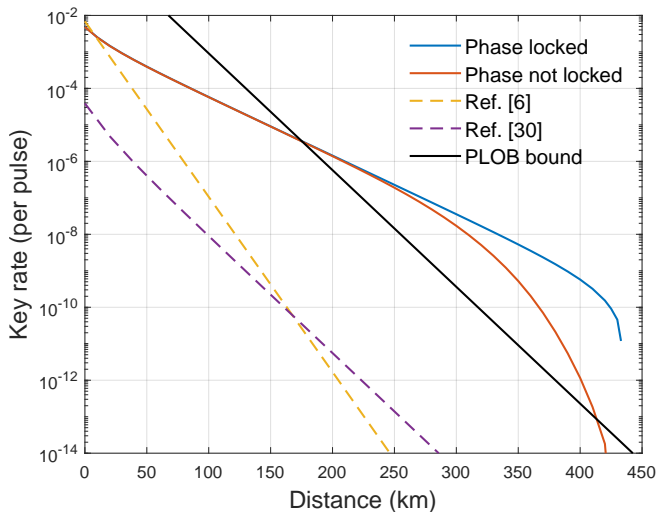


FIG. 3. Conference key rate of the AMDI-QCKA protocol in asymptotic limit with three decoy states and three users. We simulate our protocol with and without global phase locking, and compare this work with Ref.[6] and [30]. The maximum frequency difference between users’ lasers is 10 Hz and fiber phase drift rate is 3000 rad/s.

the joint GHZ measurement event. When at least one user emits a zero-photon state in two time bins and at least one user emits multiple photons, an erroneous GHZ state measurement event is obtained. There is no intrinsic error associated with the phase error rate, because with infinite number of decoy states, the joint  $N$ -photon components where  $N$  users each emits one photon can be accurately estimated. The result is consistent with the MDI-QCKA [6]. This indicates that the intrinsic nature of our protocol is the multi-photon interference.

We also compared the key rate of AMDI-QCKA with that of MDI-QCKA [6] and phase-matching QCKA [30], as shown in Fig. 3. We consider a scenario with three users employing three decoy states in the asymptotic regime. For our protocol, two cases are considered: with and without global phase locking. When the phase locking is removed, the number of pairing events is a function of distance and  $T_c$ , where  $T_c$  is globally optimized in simulation. MDI-QCKA necessitates synchronous  $N$ -multiple coincidences for a successful GHZ measurement event, and its key rate scales as  $O(\eta^N)$ . The phase-matching QCKA requires the coincidence clicks of  $N - 1$  measurement branches, and the key rate scaling is  $O(\eta^{N-1})$ . The global phase locking is necessary to phase-matching QCKA, but is not required by MDI-QCKA. With the linear scaling of the AMDI-QCKA, our protocol surpasses the bound and achieves a maximum transmission distance of over 400 km. The key rates, whether the phase is locked or not, are almost the same when  $L < 250$  km, because sufficient detection events can be found within  $T_c$ . An advantage in the key rate by approximately six orders of magnitude can be observed at 300 km. Additionally, if we set a cutoff line of  $10^{-10}$  for

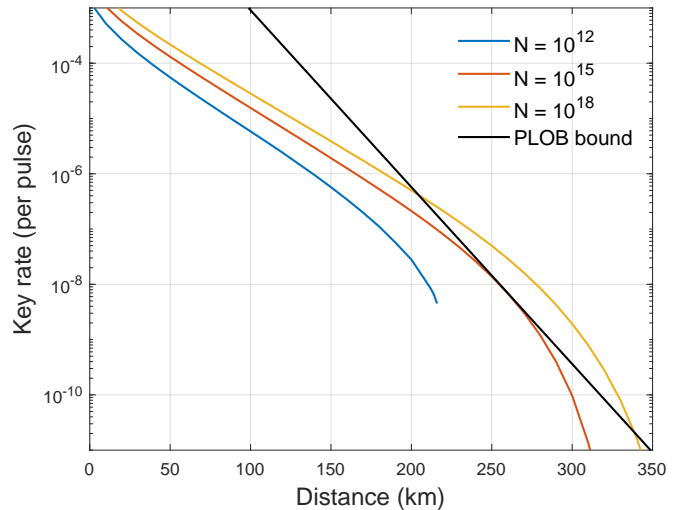


FIG. 4. Conference key rate of the AMDI-QCKA protocol in finite size regime for three users with three decoy states. The global phase locking is not utilized. We simulate the case where the number of total pulse that each user send as  $10^{12}$ ,  $10^{15}$  and  $10^{18}$ . The Chernoff bound [39] is employed for finite key analysis, and we set failure probability  $10^{-7}$ . Our protocol can break the PLOB bound in finite size regime.

real-life consideration, the transmission distance of our protocol is over 400 km, whereas the other two protocols are all below 170 km.

Finally, in Fig. 4 we show the key rate of AMDI-QCKA in finite size with three decoy states in the three-user case. The global phase locking is not utilized. The results show that even in finite size regime, our protocol still breaks the PLOB bound at 200 km, and the maximum transmission distance is over 300 km. In the finite-key regime, a desired pairing event requires multiple users to simultaneously select the intended intensity. For instance, a  $[2\nu_1, 2\nu_2, 2\nu_3]$  event requires three users to choose the decoy intensity, with its probability of occurrence being approximately proportional to  $p_{\nu_1}^2 p_{\nu_2}^2 p_{\nu_3}^2$ . By employing the click filtering method [37] to pre-exclude unwanted pairing events, such as the  $[2\nu_1, 2\nu_2, \nu_3 + \mu_3]$  event, the key rate can be further enhanced.

*Discussion.*—We propose an efficient QCKA protocol for general  $N$  users that surpasses the fundamental limit in repeaterless quantum networks. By introducing asynchronous pairing of multiple detection events as coincidence events, the postselected GHZ entanglement can be distributed. The key rate is increased to scale as  $O(\eta)$  at intercity distance, regardless of the user number in the network. In terms of security, based on postselected GHZ entanglement, the our protocol is measurement-device-independent. In the practice aspect, our protocol utilizes a cyclic interference structure with linear optics, while removing the complex global phase locking, thereby greatly simplifying the experiment complexity. Moreover, the presented key rate formula with composable security incorporates decoy state method, enhancing the applicabil-

ity in real-world scenarios. In the future, by introducing  $\mathbf{Y}$ -basis measurement to more tightly estimate the phase error rate, the six state encoding can be employed in AMDI-QCKA to further increase performance [40].

The core idea presented in this paper not only introduces new approaches for QCKA, but also has the potential for various quantum information tasks. Firstly, by employing the  $\mathbf{X}$ -basis to extract secure keys and the  $\mathbf{Z}$ -basis to estimate the phase error rate, our scheme can be adapted for quantum secret sharing. Secondly, the

AMDI-QCKA network incorporates an interference loop spanning a two-dimensional plane, which is different from the conventional one-dimensional single-chain quantum key distribution systems. This suggests possible applications in quantum sensing for precision measurements of environmental changes [41, 42]. Lastly, the structure of the AMDI-QCKA resembles the time-reversed GHZ experiment where state preparation replaces state measurements. This facilitates experiments related to Mermin's argument on the Kochen-Specker theorem [43, 44].

- 
- [1] H. J. Kimble, The quantum internet, *Nature* **453**, 1023 (2008).
- [2] S. Wehner, D. Elkouss and R. Hanson, Quantum internet: A vision for the road ahead, *Science* **362**, eaam9288 (2018).
- [3] X.-Y. Cao *et al.*, Experimental quantum e-commerce, *Sci. Adv.* **10**, eadk3258 (2024).
- [4] C.-X. Weng *et al.*, Beating the fault-tolerance bound and security loopholes for Byzantine agreement with a quantum solution, *Research* **6**, 0272 (2023).
- [5] S. Bose, V. Vedral and P. L. Knight, Multiparticle generalization of entanglement swapping, *Phys. Rev. A* **57**, 822 (1998).
- [6] Y. Fu, H.-L. Yin, T.-Y. Chen and Z.-B. Chen, Long-distance measurement-device-independent multiparty quantum communication, *Phys. Rev. Lett.* **114**, 090501 (2015).
- [7] M. Proietti *et al.*, Experimental quantum conference key agreement, *Sci. Adv.* **7**, eabe0395 (2021).
- [8] J.-W. Pan *et al.*, Multiphoton entanglement and interferometry, *Rev. Mod. Phys.* **84**, 777 (2012).
- [9] K. Chen and H.-K. Lo, Multi-partite quantum cryptographic protocols with noisy GHZ States, *Quantum Inf. Comput.* **7**, 689 (2007).
- [10] M. Epping, H. Kampermann, D. Bruß *et al.*, Multipartite entanglement can speed up quantum key distribution in networks, *New J. Phys.* **19**, 093012 (2017).
- [11] J. Ribeiro, G. Murta and S. Wehner, Fully device-independent conference key agreement, *Phys. Rev. A* **97**, 022307 (2018).
- [12] X.-Y. Cao, J. Gu, Y.-S. Lu, H.-L. Yin and Z.-B. Chen, Coherent one-way quantum conference key agreement based on twin field, *New J. Phys.* **23**, 043002 (2021).
- [13] E. Kaur, M. M. Wilde and A. Winter, Fundamental limits on key rates in device-independent quantum key distribution, *New J. Phys.* **22**, 023039 (2020).
- [14] T. Holz, H. Kampermann and D. Bruß, Genuine multipartite Bell inequality for device-independent conference key agreement, *Phys. Rev. Res.* **2**, 023251 (2020).
- [15] Z. Li *et al.*, Finite-key analysis for quantum conference key agreement with asymmetric channels, *Quantum Sci. Technol.* **6**, 045019 (2021).
- [16] K. Horodecki, M. Winczewski and S. Das, Fundamental limitations on the device-independent quantum conference key agreement, *Phys. Rev. A* **105**, 022604 (2022).
- [17] F. Grasselli, H. Kampermann and D. Bruß, Finite-key effects in multipartite quantum key distribution protocols, *New J. Phys.* **20**, 113014 (2018).
- [18] J.-L. Bai, Y.-M. Xie, Z. Li, H.-L. Yin and Z.-B. Chen, Post-matching quantum conference key agreement, *Opt. Express* **30**, 28865 (2022).
- [19] A. Pickston *et al.*, Conference key agreement in a quantum network, *npj Quantum Inf.* **9**, 82 (2023).
- [20] S. Liu *et al.*, Experimental demonstration of multiparty quantum secret sharing and conference key agreement, *NPJ Quantum Inf.* **9**, 92 (2023).
- [21] A. Philip, E. Kaur, P. Bierhorst and M. M. Wilde, Multipartite intrinsic non-locality and device-independent conference key agreement, *Quantum* **7**, 898 (2023).
- [22] S. Das, S. Bäuml, M. Winczewski and K. Horodecki, Universal limitations on quantum key distribution over a network, *Phys. Rev. X* **11**, 041016 (2021).
- [23] S. Pirandola, General upper bound for conferencing keys in arbitrary quantum networks, *IET Quantum Commun.* **1**, 22 (2020).
- [24] S. Pirandola, R. Laurenza, C. Ottaviani and L. Banchi, Fundamental limits of repeaterless quantum communications, *Nat. Commun.* **8**, 1 (2017).
- [25] M. Lucamarini, Z. L. Yuan, J. F. Dynes and A. J. Shields, Overcoming the rate-distance limit of quantum key distribution without quantum repeaters, *Nature* **557**, 400 (2018).
- [26] Y.-M. Xie *et al.*, Breaking the rate-loss bound of quantum key distribution with asynchronous two-photon interference, *PRX Quantum* **3**, 020315 (2022).
- [27] P. Zeng, H. Zhou, W. Wu and X. Ma, Mode-pairing quantum key distribution, *Nat. Commun.* **13**, 3903 (2022).
- [28] H.-K. Lo, M. Curty and B. Qi, Measurement-device-independent quantum key distribution, *Phys. Rev. Lett.* **108**, 130503 (2012).
- [29] C. Ottaviani, C. Lupo, R. Laurenza and S. Pirandola, Modular network for high-rate quantum conferencing, *Commun. Phys.* **2**, 118 (2019).
- [30] S. Zhao *et al.*, Phase-matching quantum cryptographic conferencing, *Phys. Rev. Appl.* **14**, 024010 (2020).
- [31] F. Grasselli, H. Kampermann and D. Bruß, Conference key agreement with single-photon interference, *New J. Phys.* **21**, 123002 (2019).
- [32] C.-L. Li *et al.*, Breaking universal limitations on quantum conference key agreement without quantum memory, *Commun. Phys.* **6**, 122 (2023).
- [33] G. Carrara, G. Murta and F. Grasselli, Overcoming Fundamental Bounds on Quantum Conference Key Agree-

- ment, *Phys. Rev. Appl.* **19**, 064017 (2023).
- [34] Y.-S. Lu *et al.*, Efficient quantum digital signatures without symmetrization step, *Opt. Express* **29**, 10162 (2021).
- [35] H.-K. Lo, X. Ma and K. Chen, Decoy state quantum key distribution, *Phys. Rev. Lett.* **94**, 230504 (2005).
- [36] X.-B. Wang, Beating the photon-number-splitting attack in practical quantum cryptography, *Phys. Rev. Lett.* **94**, 230503 (2005).
- [37] L. Zhou *et al.*, Experimental quantum communication overcomes the rate-loss limit without global phase tracking, *Phys. Rev. Lett.* **130**, 250801 (2023).
- [38] H.-T. Zhu *et al.*, Experimental Mode-Pairing Measurement-Device-Independent Quantum Key Distribution without Global Phase Locking, *Phys. Rev. Lett.* **130**, 030801 (2023).
- [39] H.-L. Yin *et al.*, Tight security bounds for decoy-state quantum key distribution, *Sci. Rep.* **10**, 14312 (2020).
- [40] Z.-H. Wang *et al.*, Tight finite-key analysis for mode-pairing quantum key distribution, *Commun. Phys.* **6**, 265 (2023).
- [41] N. J. Lindsey, T. C. Dawe and J. B. Ajo-Franklin, Illuminating seafloor faults and ocean dynamics with dark fiber distributed acoustic sensing, *Science* **366**, 1103 (2019).
- [42] S.-R. Zhao *et al.*, Field demonstration of distributed quantum sensing without post-selection, *Phys. Rev. X* **11**, 031009 (2021).
- [43] N. D. Mermin, Simple unified form for the major no-hidden-variables theorems, *Phys. Rev. Lett* **65**, 3373 (1990).
- [44] S. Kochen and E. P. Specker, The Problem of Hidden Variables in Quantum Mechanics, *J. Math. Mech.* **17**, 59 (1967).
- [45] D. Gottesman, H.-K. Lo, N. Lütkenhaus and J. Preskill, Security of quantum key distribution with imperfect devices, *Quantum Inf. Comput.* **4**, 325 (2004).
- [46] D. Bruß, Optimal Eavesdropping in Quantum Cryptography with Six States, *Phys. Rev. Lett.* **81**, 3018 (1998).
- [47] A. Vitanov, F. Dupuis, M. Tomamichel and R. Renner, Chain Rules for Smooth Min- and Max-Entropies, *IEEE Trans. Inf. Theory* **59**, 2603 (2013).
- [48] M. Tomamichel, C. C. W. Lim, N. Gisin and R. Renner, Tight finite-key analysis for quantum cryptography, *Nat. Commun.* **3** (2012).
- [49] M. Curty *et al.*, Finite-key analysis for measurement-device-independent quantum key distribution, *Nat. Commun.* **5** (2014).
- [50] X. Ma and M. Razavi, Alternative schemes for measurement-device-independent quantum key distribution, *Phys. Rev. A* **86**, 062319 (2012).

**I. SUPPLEMENTAL MATERIAL FOR “REPEATER-LIKE ASYNCHRONOUS  
MEASUREMENT-DEVICE-INDEPENDENT QUANTUM CONFERENCE KEY AGREEMENT”**

**II. PAIRING ALGORITHM**

In this section, we introduce an example of the pairing algorithm designed for AMID-QCKA. We adopt a pairing strategy where the  $N$  nearest click events occurring at  $N$  different ports are paired. There may exist more efficient pairing strategies. For security, the pairing strategy needs to meet two conditions [37]. Firstly, from Eve’s point of view, the pairing results should be random and independent of the basis. Secondly, the total intensity of the pair event is randomly decided, and is independent of Eve’s operation.

---

**Algorithm 1:** Pairing algorithm for the AMDI-QCKA

---

**Input:** Detection result sequence  $D = \{T, P, f\}$ , where  $T$  is the time of the click event,  $P \in \{P_1, P_2, \dots, P_N\}$  is the detection port,  $f = 1(0)$  denotes the click event has been paired (not paired).

**Output:** The set of pairing event  $\mathcal{P} = \{\mathcal{D}\}$ , where  $\mathcal{D}$  includes  $N$  click events at  $N$  different ports that are paired.

```

1 Initialize the pairing result sequence  $\mathcal{P}$ , set  $Start\_index = 1$ ,  $Repeat\_entry = 0$ ,  $j = 1$ ;
2 while  $Start\_index \leq length(D)$  do
3   for  $t = Start\_index : length(D)$  do
4     if  $D[t].T > D[Start\_index].T + T_c$  // Verify whether time interval is larger than  $T_c$ 
5       then
6         Set the index of the last unused click event as  $Start\_index$ 
7         Break
8       end
9     if  $D[t].f = 0$  then
10       $i = Get\_DetectionPort(D[t].P)$ 
11      if  $\mathcal{P}[j].\mathcal{D}[i]$  is empty then
12         $\mathcal{P}[j].\mathcal{D}[i] = D[t]$  // Assign the click event  $D[t]$  to pair event  $\mathcal{P}[j]$ 
13         $D[t].f = 1$ 
14      else if  $Repeat\_flag = 0$  then
15         $Repeat\_entry = t$  // Record the unused click event
16         $Repeat\_flag = 1$ 
17      end
18    end
19    if  $\mathcal{P}[j]$  include detection events of all ports then
20      The  $j$ -th pairing event has been obtained
21       $j = j + 1$ 
22      if  $Repeat\_flag = 1$  then
23         $Start\_index = Repeat\_entry$ 
24      else
25        Set  $Start\_index$  to the last click event of  $P[j]$ 
26        Break
27      end
28    end
29  end
30 end

```

---

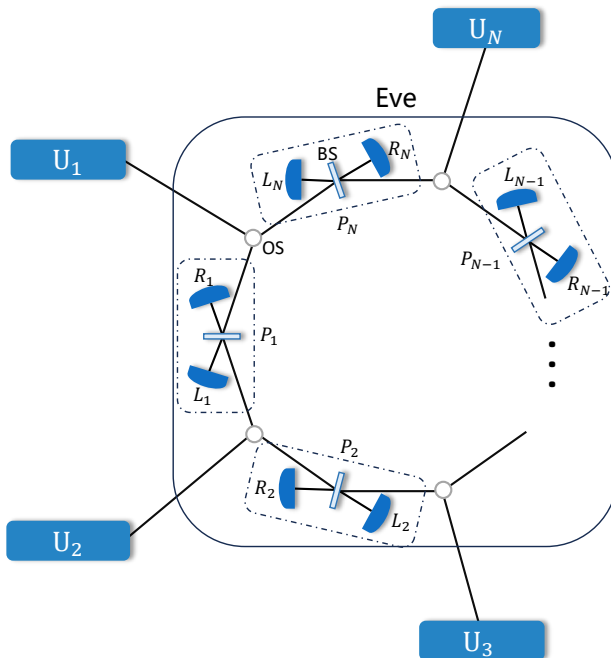


FIG. 5. The schematic diagram for the virtual protocols. There are  $N$  users  $U_1, U_2, \dots, U_N$ . The untrusted relay Eve is expected to consist of  $N$  detection ports  $P_1, P_2, \dots, P_N$ , and each port  $P_i$  includes a 50/50 beam splitter, right detector  $R_i$  and left detector  $L_i$ . Eve is expected to utilize optical switches (OS) to control the detection port where interference occurs. For the practical protocol in the main text, with the post-selection method, we can replace the OS with  $1 \times 2$  beam splitters.

### III. SECURITY PROOF

The basis of QCKA is that all legitimate users share almost perfect multiparty entanglement states. If multiparty entanglement states are shared, because the monogamy of entanglement, the users can obtain secure conference keys by measuring their states. Assume  $N$  users each prepare entangled state which contains a local qubit and an optical mode. Based on the entanglement swapping concept, we assume that each user prepares a Bell state consist of a virtual qubit and an optical mode. They send the optical mode to untrusted relay to perform the GHZ state measurement and post-select the successful GHZ state measurement events [6], leaving the local qubits to be entangled.

Similar to the security prove for the asynchronous MDI-QKD [37], here we provide the security proof for the AMDI-QCKA by using the entanglement swapping argument. We start from virtual protocols, which can be reduced to the practical protocol described in the main text.

**Virtual protocol 1.** (i) Each user  $U_i$  ( $i \in \{1, 2, \dots, N\}$ ) prepares an entangle state  $|\phi\rangle_i$ :  $|\phi\rangle_i = \sqrt{\alpha}|+z\rangle_{A_i}|1\rangle_{a_i} + \sqrt{1-\alpha}|-z\rangle_{A_i}|0\rangle_{a_i}$ , where  $|\pm z\rangle$  denote the two eigenstates of the Pauli  $Z$  operator  $\sigma_Z$ ,  $|0\rangle$  and  $|1\rangle$  are the zero and single-photon state, respectively, the superscript  $e(l)$  represents earlier (latter),  $A_i(a_i)$  denotes the local qubit (optical mode), respectively, and  $0 < \alpha < 1$ . We also have two eigenstates in the  $\mathbf{X}$  basis  $|\pm x_\varphi\rangle = (|+z\rangle \pm e^{i\varphi}|-z\rangle)/\sqrt{2}$ , where  $\varphi \in [0, 2\pi)$  is the relative phase. The users keep  $A_i^e$  and  $A_i^l$  in the local quantum memory. At time bin  $T = cN + i$  ( $c \in \mathbb{N}_0$ ),  $U_i$  and  $U_{i+1}$  ( $i \neq 1$ ) send optical modes  $a_i$  and  $a_{i+1}$  respectively to the untrusted relay, Eve (when  $i = N$ ,  $U_N$  and  $U_1$  send  $a_N$  and  $a_1$ ). They repeat for multiple rounds to accumulate sufficient data. (ii) Eve is expected to perform single-photon interference measurement on incoming optical modes. At time bin  $T = cN + i$  ( $i \neq N$ ),  $a_i$  interference with  $a_{i+1}$  at detection port  $P_i$ , and  $a_N$  interference with  $a_1$  at detection port  $P_N$ . A successful click event is obtained when one and only one detector clicks. Eve announces the click time bin and the corresponding detector. Each user  $U_i$  labels the optical mode where  $P_{i-1}$  ( $P_i, i \neq 1$ ) click as  $a_i^e$  ( $a_i^l$ ) and label the local qubit as  $A_i^e$  ( $A_i^l$ ).  $U_1$  label  $a_1^e$  ( $a_1^l$ ) and  $A_1^e$  ( $A_1^l$ ) where  $P_N$  ( $P_1$ ) clicks, as shown in Fig. 6. (iii) The participants randomly pair  $N$  time bins with successful click events that occur at  $N$  different detection ports as a successful asynchronous GHZ measurement event. They identify the corresponding GHZ state according to the clicked detector. For each pairing event,  $U_i$  performs a controlled-NOT operation on  $A_i^l$  controlled by  $A_i^e$ . They measure  $A_i^l$  in the  $\mathbf{Z}$ -basis, and keep  $A_i^e$  if their measurement results are all  $-1$ . Afterwards, the kept qubits  $A_1^e, A_2^e, \dots, A_N^e$  establish entanglement. (iv) Each user randomly chooses the  $\mathbf{Z}$  and  $\mathbf{X}$ -bases to measure the qubits  $A_1^e, A_2^e, \dots, A_N^e$  and obtains the corresponding bit values. Based on the detector click information, the users decide “whether to flip the bit value. (v) All the users publish

	$U_1$	$U_2$	$U_3$	...	$U_{N-1}$	$U_N$
$P_N$	$a_1^e$					$a_N^l$
$P_1$	$a_1^l$	$a_2^e$				
$P_2$		$a_2^l$	$a_3^e$			
...						
$P_{N-1}$					$a_{N-1}^l$	$a_N^e$

FIG. 6. The relationship between the users and the detection ports where interference occurs. For instance, optical mode from  $U_1$  and  $U_N$  interferes at  $P_N$  are labeled  $a_1^e$  and  $a_N^l$ , respectively, while other users have no association with  $P_N$ . A paired event consists of  $N$  detection events occurring in  $N$  different ports.

the basis information through an authenticated classical channel. They use the data in the  $\mathbf{X}$ -basis to estimate the phase error rate, and the data in the  $\mathbf{Z}$ -basis to generate the conference key. By implementing a multipartite error correction and privacy amplification algorithm, they extract the final secret conference key.

Here, we notice that the pairing and the controlled-NOT operation of the users commute with the single-photon interference measurement of Eve. For example, after receiving the optical mode, Eve stores them in quantum memories, and can perform the single-photon interference measurement at any time. The users may perform the local operation without influencing the interference measurement result. Therefore, we can exchange the order of the steps (iii) and (iv) with (ii), keeping the security unchanged. Therefore we have virtual protocol 2.

**Virtual protocol 2.** (i) Through an authenticated classical channel, they negotiate to randomly pair  $N$  time bins  $T = cN + i$  with different  $i$ . Each user  $U_i$  prepares entangled states  $|\phi\rangle_i^e = \sqrt{\alpha}|+z\rangle_{A_i^e}|1\rangle_{a_i^e} + \sqrt{1-\alpha}| -z\rangle_{A_i^e}|0\rangle_{a_i^e}$  and  $|\phi\rangle_i^l = \sqrt{\alpha}|+z\rangle_{A_i^l}|1\rangle_{A_i^l} + \sqrt{1-\alpha}| -z\rangle_{A_i^l}|0\rangle_{A_i^l}$ . They perform the controlled-NOT operation and measure the latter qubit in the  $\mathbf{Z}$ -basis. At time bin  $T = cN + i$ ,  $U_i$  and  $U_{i+1}$  send  $a_i^l$  and  $a_{i+1}^e$  respectively to the measurement node. (ii) Eve performs single-photon interference measurement and announces the successful click events. The relation between the users and the port of interference is the same as virtual protocol 1. (iii) The users identify which specific GHZ state was measured according to the click events at each detection port. Steps (iv) and (v) are the same as those in the virtual protocol 1.

In virtual protocol 2, although Eve has the pairing information, Eve cannot eavesdrop the secret keys without being found. The  $\mathbf{X}$  and  $\mathbf{Z}$ -bases are randomly chosen by the users and unknown to Eve before Eve broadcasts the click information, and Eve's operation will give rise to phase error rate. Once the basis choice information is unknown to Eve, the security can be guaranteed. Thus the pre-pairing of virtual protocol 2 does not change the security of the protocol. However, the post-pairing in virtual protocol 1 can significantly increase the valid data.

Virtual protocol 2 is actually the entanglement-swapping process. In step (i), the joint state that each user  $U_i$  prepares is

$$|\phi\rangle_i^e \otimes |\phi\rangle_i^l = \alpha|+z+z\rangle_{A_i^e A_i^l}|11\rangle_{a_i^e a_i^l} + \sqrt{\alpha(1-\alpha)}|+z-z\rangle_{A_i^e A_i^l}|10\rangle_{a_i^e a_i^l} \\ + \sqrt{\alpha(1-\alpha)}|-z+z\rangle_{A_i^e A_i^l}|01\rangle_{a_i^e a_i^l} + (1-\alpha)|-z-z\rangle_{A_i^e A_i^l}|00\rangle_{a_i^e a_i^l}. \quad (3)$$

After the controlled-NOT operation and measure  $A_i^l$ , the quantum state of  $U_i$  is

$$|\Phi\rangle_{A_i^e a_i^e a_i^l} = \frac{1}{\sqrt{2}} e^{i2\varphi} \left( |+z\rangle_{A_i^e} |10\rangle_{a_i^e a_i^l} + |-z\rangle_{A_i^e} |01\rangle_{a_i^e a_i^l} \right) \\ = \frac{1}{\sqrt{2}} \left( |+x\rangle_{A_i^e} \frac{|10\rangle_{a_i^e a_i^l} + e^{i\varphi}|01\rangle_{a_i^e a_i^l}}{\sqrt{2}} + |-x\rangle_{A_i^e} \frac{|10\rangle_{a_i^e a_i^l} - e^{i\varphi}|01\rangle_{a_i^e a_i^l}}{\sqrt{2}} \right). \quad (4)$$

After the GHZ state measurement by Eve, the users' local qubits are entangled.

The measurement of  $A_i^e$  can be preceded to step (i) because the measurement operation commutes other steps. The entanglement-based protocol can be equivalently transferred to prepare-and-measure protocol. When the measurement outcome of  $A_i^l$  is  $|+z\rangle$  ( $|-z\rangle$ ),  $U_i$  prepares the state  $|10\rangle_{a_i^e a_i^l}$  ( $|01\rangle_{a_i^e a_i^l}$ ). When the outcome is  $|+x\rangle$  ( $|-x\rangle$ ),  $U_i$  prepares  $\frac{1}{\sqrt{2}}(|10\rangle_{a_i^e a_i^l} + e^{i\varphi}|01\rangle_{a_i^e a_i^l})$  ( $\frac{1}{\sqrt{2}}(|10\rangle_{a_i^e a_i^l} - e^{i\varphi}|01\rangle_{a_i^e a_i^l})$ ). Thus, we have the virtual protocol 3, where the users directly prepare optical modes instead of entangled states.

**Virtual protocol 3.** Through an authenticated classical channel, the  $N$  users first negotiate to randomly pair  $N$  time bins with different  $i$ . Each user  $U_i$  randomly chooses  $\mathbf{X}$  or  $\mathbf{Z}$ -basis. If the user chooses  $\mathbf{Z}$  basis, they randomly prepare optical modes  $|10\rangle_{a_i^e a_i^l}$  and  $|01\rangle_{a_i^e a_i^l}$ . If they choose  $\mathbf{X}$  basis, the user randomly prepares state  $\frac{1}{2}(|10\rangle_{a_i^e a_i^l} \pm e^{i\phi}|01\rangle_{a_i^e a_i^l})$ .  $U_i$  and  $U_{i+1}$  send  $a_i^l$  and  $a_{i+1}^e$  respectively to the measurement node at time bin  $T = cN + i$ . The following steps, including single-photon interference measurement, parameter estimation, error correction and privacy amplification are the same as virtual protocol 2.

In real implementation, the phase-randomized coherent source can be utilized as replacement because of the difficulty and low efficiency in directly preparing single-photon states. With a random global phase of the coherent pulse, from the view of Eve, the joint state that each user send is Fock state. Using decoy state method [35, 36] and tagged model [45], one can effectively estimate the amount of single-photon events and obtain secure secret key. Therefore we have virtual protocol 4, where the users prepare phase-randomized coherent state instead of single-photon state.

**Virtual protocol 4.** The  $N$  users first negotiate to randomly pair  $N$  time bins with different  $i$ . Each user  $U_i$  randomly chooses  $\mathbf{X}$  or  $\mathbf{Z}$ -basis with probabilities  $p_z$  and  $p_x$ , respectively. They randomly prepare quantum states  $|e^{i\theta}\sqrt{k}\rangle_{a_i^e}|0\rangle_{a_i^l}$  and  $|0\rangle_{a_i^e}|e^{i\theta}\sqrt{k}\rangle_{a_i^l}$  in the  $\mathbf{Z}$ -basis, and  $\frac{1}{2}(|\sqrt{k}\rangle_{a_i^e}|0\rangle_{a_i^l} \pm e^{i(\theta_l - \theta_e)}|0\rangle_{a_i^e}|\sqrt{k}\rangle_{a_i^l})$  in the  $\mathbf{X}$ -basis, where  $\theta \in \{0, 2\pi\}$  is the global random phase. The following steps, are the same as virtual protocol 3.

There are two differences between the virtual protocol 4 and the practical protocol in the main text. First, the pairing information is pre-determined by the users in virtual protocol 4, but in the practical protocol it is determined by the detection information announced by Eve. In both cases each user sends a train of coherent states with random phase and random intensity from the view of Eve. Eve obtains same classical and quantum information in two protocols. The random basis and the bit information is determined by the intensity of the pairing event and the phase difference between two paired optical pulses. Even if Eve can control the pairing result, the bit information is still inaccessible, because the modulated phase information is stored in the user's local classical memory. In addition, as long as the pairing result is no concern with the basis information, Eve can not obtain extra basis information. Any attacks from Eve will be discovered with increased phase error rate. Therefore, the users can always utilize post-pair method to increase the valid data, with security level equal to the virtual protocol.

In addition, in virtual protocol 4, Eve is expected to actively control the detection port where interference occurs at each time bin. In practice, Eve's operation is not restricted. Eve can arbitrarily control the detection port and declare the measurement result. However, this inevitably gives rise to phase error rate. Therefore, we can adopt the post-selection strategy. All the users simultaneously send phase-randomized coherent state. When single click event occurs at detection port  $P_i$ , one can post-select this click event as a result of interference of  $a_i^l$  and  $a_{i+1}^e$ , corresponding to the practical protocol.

In conclusion, we have proven that the security of the AMDI-QCKA protocol in the main text is equivalent to that of the entanglement-based protocol.

#### IV. COMPOSABLE SECURITY

Here we prove the composable security of the AMDI-QCKA protocol. We first give the definitions of the security criteria for the QCKA. A QCKA protocol is  $\varepsilon_{\text{cor}}$ -correct if

$$\Pr(\exists i \in \{2, \dots, n\}, \text{s.t. } \mathbf{S}_1 \neq \mathbf{S}_i) \leq \varepsilon_{\text{cor}}, \quad (5)$$

where  $S_i$  ( $i \in \{1, 2, \dots, n\}$ ) is the final key of  $U_i$ . A QCKA protocol is called  $\varepsilon_{\text{sec}}$ -secret if

$$p_{\text{pass}} D \left( \rho_{\mathbf{S}_1, E}, \sum_{\mathbf{S}_1} \frac{1}{|\mathbf{S}_1|} |\mathbf{S}_1\rangle\langle\mathbf{S}_1| \otimes \sigma_E \right) \leq \varepsilon_{\text{sec}}, \quad (6)$$

where  $p_{\text{pass}}$  is the probability of passing the protocol,  $D(\cdot, \cdot)$  is the trace distance,  $\sigma_E$  is the system of the eavesdropper.

Then, we provide the composable security proof for the AMDI-QCKA protocol and the final key rate formula.

**Theorem 1.** *The AMDI-QCKA protocol is  $\varepsilon_{\text{cor}}$ -correct.*

*Proof:* Let  $\{\text{EC}_i\}_{i=2}^n$  be a set of error correction (EC) protocols,  $P_{\mathbf{X}\mathbf{K}}$  is a probability distribution, where where  $k_i$  is the guess of  $x$  of the  $i$ -th user. Any set of EC protocols, which is  $\varepsilon_{\text{cor}}$ -secure, satisfies  $\Pr(\exists i \in \{2, \dots, n\}, \text{s.t. } \mathbf{x} \neq \mathbf{k}_i) \leq \varepsilon_{\text{cor}}$ . According to Theorem 2 in Ref. [17], given  $P_{\mathbf{X}\mathbf{K}}$ , there exists a one-way EC protocol with  $\varepsilon_{\text{cor}}$ -fully secure on  $P_{\mathbf{X}\mathbf{K}}$  with information leakage  $\text{leak}_{\text{EC}} + \log_2 \frac{2(N-1)}{\varepsilon_{\text{cor}}}$ . Therefore, the  $\varepsilon_{\text{cor}}$ -correctness of the AMDI-QCKA protocol can be guaranteed during the error correction process.

**Theorem 2.** *The QCKA protocol defined in the main text is  $\varepsilon_{\text{sec}}$ -secret if the key length  $l$  satisfies Eq.(2) in the main text.*

*Proof.* The quantum leftover hashing lemma [46] shows that if  $U_1$  map the raw key  $\mathbf{Z}$  to the final key  $\mathbf{S}$  and extracts a string of length  $l$  utilizing a random universal<sub>2</sub> hash function, for any positive  $\epsilon$ , we have

$$\epsilon_{\text{sec}} \geq \frac{1}{2} \sqrt{2^{l-H_{\min}^{\epsilon}(\mathbf{Z}|\mathbf{E}')}} + 2\epsilon, \quad (7)$$

where  $\mathbf{E}'$  is the auxiliary system of Eve after error correction, and  $H_{\min}^{\epsilon}(\mathbf{Z}|\mathbf{E}')$  can be bounded by

$$H_{\min}^{\epsilon}(\mathbf{Z}|\mathbf{E}') \geq H_{\min}^{\epsilon}(\mathbf{Z}|\mathbf{E}) - \text{leak}_{\text{EC}} - \log_2 \frac{2(N-1)}{\epsilon_{\text{cor}}}, \quad (8)$$

where  $\mathbf{E}$  is the auxiliary system of Eve before error correction.

To bound the term  $H_{\min}^{\epsilon}(\mathbf{Z}|\mathbf{E})$ , using the chain-rule inequality for smooth entropies [37, 47], we have

$$\begin{aligned} H_{\min}^{\epsilon}(\mathbf{Z}|\mathbf{E}) &\geq H_{\min}^{\epsilon'+2\epsilon_e+(\hat{\epsilon}+2\hat{\epsilon}'+\hat{\epsilon}'')}(\mathcal{Z}_0\mathcal{Z}_N\mathcal{Z}_{\text{rest}}|\mathbf{E}) \\ &\geq s_0^z + H_{\min}^{\epsilon_e}(\mathcal{Z}_N|\mathcal{Z}_0\mathcal{Z}_{\text{rest}}|\mathbf{E}) - 2\log_2(2/\epsilon'\hat{\epsilon}) \end{aligned} \quad (9)$$

where  $\epsilon = \epsilon' + 2\epsilon_e + (\hat{\epsilon} + 2\hat{\epsilon}' + \hat{\epsilon}'')$ ,  $\mathcal{Z}_0$ ,  $\mathcal{Z}_N$  and  $\mathcal{Z}_{\text{rest}}$  represents the bits when  $U_1$  send vacuum state, the  $N$  users each sends a single-photon state and the rest cases, respectively. We used the fact that  $H_{\min}^{\epsilon'}(\mathcal{Z}_{\text{rest}}|\mathcal{Z}_0\mathbf{E}) \geq 0$  and  $H_{\min}^{\epsilon''}(\mathcal{Z}_0|\mathbf{E}) \geq H_{\min}(\mathcal{Z}_0) = s_0^z$ . Because the the single-photon component prepared in the  $\mathbf{Z}$ -basis and  $\mathbf{X}$ -basis are mutually unbiased, we can use phase error rate  $\phi_N^z$  to quantify the minimum smooth entropy using the entropic uncertainty relations [48, 49]:

$$\begin{aligned} H_{\min}^{\epsilon_e}(\mathcal{Z}_N|\mathcal{Z}_0\mathcal{Z}_{\text{rest}}|\mathbf{E}) &\geq s_N^z - H_{\max}^{\epsilon_e}(\mathcal{X}_N^1|\mathcal{X}_N^2\dots\mathcal{X}_N^N) \\ &\geq s_N^z[1 - H_2(\phi_N^z)], \end{aligned} \quad (10)$$

where  $\mathcal{X}_N^i$  represents the  $\mathbf{X}$ -basis string of  $U_i$  when the users hypothetically measure the joint  $N$ -photon state in the  $\mathbf{X}$ -basis instead of  $\mathbf{Z}$ -basis when each user sends a single-photon state. Finally, by choosing  $\hat{\epsilon}' = \hat{\epsilon}'' = 0$ , we have the final key rate formula:

$$l \geq s_0^z + s_N^z[1 - H_2(\phi_N^z)] - \text{leak}_{\text{EC}} - \log_2 \frac{2(N-1)}{\epsilon_{\text{cor}}} - 2\log_2 \frac{2}{\epsilon'\hat{\epsilon}} - 2\log_2 \frac{1}{2\epsilon_{\text{PA}}}, \quad (11)$$

where the overall security  $\epsilon_{\text{tot}}$  is defined as:  $\epsilon_{\text{tot}} = \epsilon_{\text{sec}} + \epsilon_{\text{cor}}$ ,  $\epsilon_{\text{sec}} = 2(\epsilon' + 2\epsilon_e + \hat{\epsilon}) + \epsilon_0 + \epsilon_N + \epsilon_{\beta} + \epsilon_{\text{PA}}$ ,  $\epsilon_0$ ,  $\epsilon_N$  and  $\epsilon_{\beta}$  are the failure probabilities in estimating the terms of  $s_0^z$ ,  $s_N^z$ , and  $\phi_N^z$ . Specially, in finite case with three users and three decoy states, we have  $\epsilon_0 = 4\epsilon$ ,  $\epsilon_3 = 15\epsilon$  with  $\epsilon$  is the failure probability of Chernoff bound. In simulation, we set all security parameters to the same value  $\epsilon = 10^{-7}$ .

## V. DECOY STATE ESTIMATION

### A. $N$ users with infinite decoys

To ensure the security of the the AMDI-QCKA protocol, we employ the decoy state method. Leveraging the tagged model, secure secret keys can be distilled from the joint  $N$ -photon component. Initially, we address the general scenario where there are infinite number of decoy states with  $N$  users. Subsequently, we present detailed formula for the specific 3 and 4-user cases. Finally, the three-decoy state formulas with three users are provided.

With infinite number of decoy states, we assume the number of joint  $N$ -photon component can be accurately estimated. Below we focus on symmetric case, where the users randomly choose intensity from the same setting  $\{\mu, \nu, \omega, \dots\}$ , the  $[\mu, \mu, \dots, \mu]$  events are assigned to  $\mathbf{Z}$ -basis,  $[2\nu, 2\nu, \dots, 2\nu]$  events are assigned to  $\mathbf{X}$ -basis, and other events are used in parameter estimation. The final key rate formula is

$$R = \tilde{Y}_N^z [1 - H_2(\phi_N^z)] - \text{leak}_{\text{EC}}, \quad (12)$$

where  $\tilde{Y}_N^{z(x)} := s_N^{z(x)}/\mathcal{N}$  is defined as the probability of obtaining a joint  $N$ -photon event in the  $\mathbf{Z}(\mathbf{X})$ -basis per pulse,  $\mathcal{N}$  is the total number of pulses transmitted by each user,  $s_N^{z(x)}$  denotes the number of joint  $N$ -photon event,  $\phi_N^z$  denotes

the phase error rate,  $\text{leak}_{\text{EC}} = \max_{2 \leq i \leq N} [H_2(E_{1,i}^z)] f \tilde{Q}_{[\mu, \mu, \dots, \mu]}^z$  is the information leakage,  $\tilde{Q}_{[\mu, \mu, \dots, \mu]}^z := n_{[\mu, \mu, \dots, \mu]}^{z(x)} / \mathcal{N}$  is the the probability of obtaining a  $\mathbf{Z}$ -basis event per pulse.  $\tilde{Y}_N^z$  can be given as

$$\tilde{Y}_N^z = p_{\text{pair}} (p_\mu p_o \mu e^{-\mu} p_{\text{det}}^-)^N \sum_{i=1, a_i^e + a_i^l = 1}^N \prod_{i=1}^N \frac{y_{a_{i+1}^e a_i^l}^{P_i}}{q_{\text{tot}}^{P_i}} \quad (13)$$

where  $p_{\text{det}}^- = \{[1 - (1 - e^{-\bar{\mu}\eta})] (1 - p_d)^2\}^{N-1}$  represents the other  $N - 1$  ports have no click events,  $\bar{\mu}$  is the mean photon number from each user,  $\eta$  is the transmittance from user to Eve,  $p_{\text{pair}}$  is the probability of obtaining a pairing event given in Eq. (56),  $a_i^{e(l)} \in \{0, 1\}$  is the number of incident photon of the early (late) time of  $U_i$ ,  $q_{\text{tot}}^{P_i}$  is the probability that detection port  $P_i$  have click.  $y_{a_{i+1}^e a_i^l}^{P_i}$  is the probability of having a click in detection port  $P_i$  when  $a_{i+1}^e$  and  $a_i^l$  photons from the two input paths of the beam splitter. Due to the circulation relation,  $a_{N+1}^{e(l)}$  will be replaced with  $a_1^{e(l)}$ . For each value of  $N$ , there are  $2^N$  cases of photon number distribution in the  $\mathbf{Z}$ -basis. In symmetric channels, the loss from each user to Eve are equal, thus we assume  $y_{ab} = y_{a_2^e a_1^l}^{P_1} = y_{a_3^e a_2^l}^{P_2} = \dots = y_{a_1^e a_N^l}^{P_N}$  ( $a, b \in \{0, 1\}$ ). Therefore, for each possible  $y_{ab}$  we have

$$\begin{aligned} y_{11} &= 2p_d(1 - p_d)(1 - \eta')^2 + 2\eta'(1 - p_d)(1 - \eta) + \frac{\eta'^2}{2}(1 - p_d), \\ y_{10} &= y_{01} = 2p_d(1 - p_d)(1 - \eta') + \eta'(1 - p_d), \\ y_{00} &= 2p_d(1 - p_d), \end{aligned} \quad (14)$$

where  $p_d$  is the dark counting rate,  $\eta' = \frac{1}{2}\eta$ , and the factor  $\frac{1}{2}$  is introduce from the  $1 \times 2$  beam splitter. In the  $\mathbf{X}$ -basis, because the density matrices for the joint  $N$ -photon components in the two bases are the same, the expected ratio of different intensity settings for joint  $N$ -photon components have the following relation:

$$\frac{\tilde{Y}_N^z}{\tilde{Y}_N^x} = \frac{\mu^N e^{-N\mu} p_{[\mu, \mu, \dots, \mu]}}{(2\nu)^N e^{-2N\nu} p_{[2\nu, 2\nu, \dots, 2\nu]}}, \quad (15)$$

where  $p_{[k_1^{\text{tot}}, k_2^{\text{tot}}, \dots, k_N^{\text{tot}}]} = \sum_{k_i^e + k_i^l = k_i^{\text{tot}}} \prod_{i=1}^N p_{k_i^e} p_{k_i^l}$ , except for  $p_{[2\nu, 2\nu, \dots, 2\nu]} = \frac{2p_\nu^{2N}}{M}$ .  $\frac{2}{M}$  comes from the pairing condition  $\theta_g / \pi \bmod 2 = 0$  or  $1$ . To obtain the phase error rate  $\phi_N^z$ , we first calculate  $e_N^x$ , the bit error rate of the joint  $N$ -photon component of the  $\mathbf{X}$ -basis. In asymptotic limit  $\phi_N^z = e_N^x$ . The probability of obtaining an error event per pulse is

$$e_N^x \tilde{Y}_N^x = p_{\text{pair}} \left(\frac{2}{M}\right) (p_\nu^2 2\nu e^{-2\nu})^N \frac{1}{\prod_{i=1}^N q_{\text{tot}}^{P_i}} [(1 - e_d) \mathcal{Y}^{\text{error}} + e_d \mathcal{Y}^{\text{cor}}], \quad (16)$$

where  $e_d$  is the misalignment error of  $\mathbf{X}$ -basis,  $\mathcal{Y}^{\text{error}}$  ( $\mathcal{Y}^{\text{cor}}$ ) is the probability of obtaining an error (correct) click event given a joint  $N$ -photon states as input, which vary with the number of users. In the following, we introduce the detailed formulas for the specific three-user and four-user cases.

### B. Three users with infinite decoy states

For the specific case of  $N = 3$ , according from Eq. (12), the key rate formula can be written as:

$$R = \tilde{Y}_3^z [1 - H_2(\phi_3^z)] - \text{leak}_{\text{EC}}. \quad (17)$$

In the  $\mathbf{Z}$ -basis,  $\tilde{Y}_3^z$  can be given as:

$$\begin{aligned} \tilde{Y}_3^z &= p_{\text{pair}} (p_\mu p_o \mu e^{-\mu} p_{\text{det}}^-)^3 \sum_{a_1^e + a_1^l = 1} \sum_{a_2^e + a_2^l = 1} \sum_{a_3^e + a_3^l = 1} \left( \frac{y_{a_1^e a_3^l}^{P_3} y_{a_2^e a_1^l}^{P_1} y_{a_3^e a_2^l}^{P_2}}{q_{\text{tot}}^{P_1} q_{\text{tot}}^{P_2} q_{\text{tot}}^{P_3}} \right) \\ &= p_{\text{pair}} \frac{(p_\mu p_o \mu e^{-\mu} p_{\text{det}}^-)^3}{q_{\text{tot}}^{P_1} q_{\text{tot}}^{P_2} q_{\text{tot}}^{P_3}} (2y_{10}y_{10}y_{10} + 6y_{11}y_{10}y_{00}). \end{aligned} \quad (18)$$

The probability of obtaining a joint three photon event in the  $\mathbf{X}$ -basis is calculated using the relation between  $\tilde{Y}_3^z$  and  $\tilde{Y}_3^x$ :

$$\frac{\tilde{Y}_3^z}{\tilde{Y}_3^x} = \frac{\mu^3 e^{-3\mu} p_{[\mu,\mu,\mu]}}{8\nu^3 e^{-6\nu} p_{[2\nu,2\nu,2\nu]}}, \quad (19)$$

where  $p_{[\mu,\mu,\mu]} = 8p_\mu p_o$ ,  $p_{[2\nu,2\nu,2\nu]} = \frac{2p_\nu^6}{M}$ .

We use the GHZ state  $|\Phi_0^+\rangle$  as the reference state:

$$|\Phi_0^+\rangle = \frac{1}{\sqrt{2}}(|111\rangle + |000\rangle) = \frac{1}{2}(|+++ \rangle + |+- - \rangle + |-+ - \rangle + |--+ \rangle). \quad (20)$$

When the click detectors of  $\{P_1, P_2, P_3\}$  are  $\{L_1, L_2, L_3\}$ ,  $\{L_1, R_2, R_3\}$ ,  $\{R_1, L_2, R_3\}$  or  $\{R_1, R_2, L_3\}$ , we obtain a successful measurement event of  $|\Phi_0^+\rangle$ . The other four cases corresponding to error event. Therefore, the probability of obtaining an error event of the joint three-photon components in the  $\mathbf{X}$ -basis can be given as

$$e^x \tilde{Y}_3^x = p_{\text{pair}} \left( \frac{2}{M} \right) \frac{(2\nu e^{-2\nu} p_\nu^2)^3}{q_{\text{tot}}^{P_1} q_{\text{tot}}^{P_2} q_{\text{tot}}^{P_3}} \left[ (1 - e_d)(y^{R,R,R} + y^{R,L,L} + y^{L,R,L} + y^{L,L,R}) \right. \\ \left. + e_d(y^{L,L,L} + y^{L,R,R} + y^{R,L,R} + y^{R,R,L}) \right], \quad (21)$$

where  $y^{R(L)R(L)R(L)}$  is the probability of having detector  $R_1(L_1)$ ,  $R_2(L_2)$ ,  $R_3(L_3)$  click when input joint three-photon states in the  $\mathbf{X}$ -basis. Using the method derived in [50], they can be calculated as follows. The input joint three-photon state can be written as

$$\left[ \frac{1}{\sqrt{2}}(|10\rangle_{a_1^e a_1^l} + e^{i\theta_1}|01\rangle_{a_1^e a_1^l}) \right] \otimes \left[ \frac{1}{\sqrt{2}}(|10\rangle_{a_2^e a_2^l} + e^{i\theta_2}|01\rangle_{a_2^e a_2^l}) \right] \otimes \left[ \frac{1}{\sqrt{2}}(|10\rangle_{a_3^e a_3^l} + e^{i\theta_3}|01\rangle_{a_3^e a_3^l}) \right]. \quad (22)$$

After passing through channel with transmittance  $\eta_1, \eta_2, \eta_3$ , respectively, the state becomes a mixed state:

$$\frac{\eta^3}{8} |\psi_{111}\rangle \langle \psi_{111}| + \frac{3\eta^2(1-\eta)}{4} (|\psi_{110}\rangle \langle \psi_{110}| + |\psi_{101}\rangle \langle \psi_{101}| + |\psi_{011}\rangle \langle \psi_{011}|) \\ + \frac{3\eta(1-\eta)^2}{2} (|\psi_{100}\rangle \langle \psi_{100}| + |\psi_{010}\rangle \langle \psi_{010}| + |\psi_{001}\rangle \langle \psi_{001}|) \\ + (1-\eta)^3 |\psi_{000}\rangle \langle \psi_{000}|. \quad (23)$$

where we use the state  $|a_1^e a_1^l a_2^e a_2^l a_3^e a_3^l\rangle$  to represent photon number from different users' early (late) time bin of the joint three-photon state. The terms are:

$$|\psi_{111}\rangle_{a_1^e a_1^l a_2^e a_2^l a_3^e a_3^l} = |101010\rangle + e^{i\theta_3}|101001\rangle + e^{i\theta_2}|100110\rangle + e^{i(\theta_2+\theta_3)}|100101\rangle + e^{i\theta_1}|011010\rangle \\ + e^{i(\theta_1+\theta_3)}|011001\rangle + e^{i(\theta_1+\theta_2)}|010110\rangle + e^{i(\theta_1+\theta_2+\theta_3)}|010101\rangle, \\ |\psi_{110}\rangle_{a_1^e a_1^l a_2^e a_2^l a_3^e a_3^l} = |101000\rangle + e^{i\theta_2}|100100\rangle + e^{i\theta_1}|011000\rangle + e^{i(\theta_1+\theta_2)}|010100\rangle, \\ |\psi_{101}\rangle_{a_1^e a_1^l a_2^e a_2^l a_3^e a_3^l} = |100010\rangle + e^{i\theta_3}|100001\rangle + e^{i\theta_1}|010010\rangle + e^{i(\theta_1+\theta_3)}|010001\rangle, \\ |\psi_{011}\rangle_{a_1^e a_1^l a_2^e a_2^l a_3^e a_3^l} = |001010\rangle + e^{i\theta_3}|001001\rangle + e^{i\theta_2}|000110\rangle + e^{i(\theta_2+\theta_3)}|000101\rangle, \\ |\psi_{100}\rangle_{a_1^e a_1^l a_2^e a_2^l a_3^e a_3^l} = |100000\rangle + e^{i\theta_1}|010000\rangle, \\ |\psi_{010}\rangle_{a_1^e a_1^l a_2^e a_2^l a_3^e a_3^l} = |001000\rangle + e^{i\theta_2}|000100\rangle, \\ |\psi_{001}\rangle_{a_1^e a_1^l a_2^e a_2^l a_3^e a_3^l} = |000010\rangle + e^{i\theta_3}|000001\rangle, \\ |\psi_{000}\rangle_{a_1^e a_1^l a_2^e a_2^l a_3^e a_3^l} = |000000\rangle. \quad (24)$$

At the detection port  $P_i$ , the photon  $a_i^l$  interferes with  $a_{i+1}^e$  for  $i \neq N$ , and  $a_N^l$  interferes with  $a_1^e$  at  $P_N$ . Therefore, we can apply the following state transformation of the beam splitter (BS) where  $i \neq N$ :

$$|0\rangle_{a_i^l} |0\rangle_{a_{i+1}^e} \longrightarrow |0\rangle_{L_i} |0\rangle_{R_i}, \\ |1\rangle_{a_i^l} |1\rangle_{a_{i+1}^e} \longrightarrow (|2\rangle_{L_i} |0\rangle_{R_i} - |0\rangle_{L_i} |2\rangle_{R_i})/\sqrt{2}, \\ |1\rangle_{a_i^l} |0\rangle_{a_{i+1}^e} \longrightarrow (|1\rangle_{L_i} |0\rangle_{R_i} - |0\rangle_{L_i} |1\rangle_{R_i})/\sqrt{2}, \\ |0\rangle_{a_i^l} |1\rangle_{a_{i+1}^e} \longrightarrow (|1\rangle_{L_i} |0\rangle_{R_i} + |0\rangle_{L_i} |1\rangle_{R_i})/\sqrt{2}, \quad (25)$$

and

$$\begin{aligned}
|0\rangle_{a_N^l} |0\rangle_{a_1^e} &\longrightarrow |0\rangle_{L_N} |0\rangle_{R_N}, \\
|1\rangle_{a_N^l} |1\rangle_{a_1^e} &\longrightarrow (|2\rangle_{L_N} |0\rangle_{R_N} - |0\rangle_{L_N} |2\rangle_{R_N})/\sqrt{2}, \\
|1\rangle_{a_N^l} |0\rangle_{a_1^e} &\longrightarrow (|1\rangle_{L_N} |0\rangle_{R_N} - |0\rangle_{L_N} |1\rangle_{R_N})/\sqrt{2}, \\
|0\rangle_{a_N^l} |1\rangle_{a_1^e} &\longrightarrow (|1\rangle_{L_N} |0\rangle_{R_N} + |0\rangle_{L_N} |1\rangle_{R_N})/\sqrt{2}.
\end{aligned} \tag{26}$$

After the pulses interference at the BS of each detection port, consider that  $(\theta_1 + \theta_2 + \theta_3)/\pi \pmod{2} = 0$  (due to symmetry, we can obtain same result when  $\theta_1 + \theta_2 + \theta_3/\pi \pmod{2} = 1$ ), before they entering the detector, we have:

$$\begin{aligned}
|\psi_{111}\rangle_{L_3 R_3 L_1 R_1 L_2 R_2} &\longrightarrow \frac{1}{\sqrt{2}}(|101010\rangle + |100101\rangle + |011001\rangle + |010110\rangle) \\
&\quad + \frac{1}{2}e^{i\theta_3}(|20\rangle - |02\rangle)(|10\rangle + |01\rangle)|00\rangle + \frac{1}{2}e^{i\theta_2}(|10\rangle + |01\rangle)|00\rangle(|20\rangle - |02\rangle) \\
&\quad + \frac{1}{2}e^{i(\theta_2+\theta_3)}(|20\rangle - |02\rangle)|00\rangle(|10\rangle - |01\rangle) + \frac{1}{2}e^{i\theta_1}|00\rangle(|20\rangle - |02\rangle)(|10\rangle + |01\rangle) \\
&\quad + \frac{1}{2}e^{i(\theta_1+\theta_3)}(|10\rangle - |01\rangle)(|20\rangle - |02\rangle)|00\rangle + \frac{1}{2}e^{i(\theta_1+\theta_2)}|00\rangle(|10\rangle - |01\rangle)(|20\rangle - |02\rangle),
\end{aligned} \tag{27}$$

$$\begin{aligned}
|\psi_{110}\rangle_{L_3 R_3 L_1 R_1 L_2 R_2} &\longrightarrow \frac{1}{2}(|10\rangle + |01\rangle)(|10\rangle + |01\rangle)|00\rangle + \frac{1}{2}e^{i\theta_2}(|10\rangle + |01\rangle)|00\rangle(|10\rangle - |01\rangle) \\
&\quad + \frac{1}{\sqrt{2}}e^{i\theta_1}|00\rangle(|20\rangle - |02\rangle)|00\rangle + \frac{1}{2}e^{i(\theta_1+\theta_2)}|00\rangle(|10\rangle - |01\rangle)(|10\rangle - |01\rangle), \\
|\psi_{101}\rangle_{L_3 R_3 L_1 R_1 L_2 R_2} &\longrightarrow \frac{1}{2}(|10\rangle + |01\rangle)|00\rangle(|10\rangle + |01\rangle) + \frac{1}{\sqrt{2}}e^{i\theta_3}(|20\rangle - |02\rangle)|00\rangle|00\rangle \\
&\quad + \frac{1}{2}e^{i\theta_1}|00\rangle(|10\rangle - |01\rangle)(|10\rangle + |01\rangle) + \frac{1}{2}e^{i(\theta_1+\theta_3)}(|10\rangle - |01\rangle)(|10\rangle - |01\rangle)|00\rangle, \\
|\psi_{011}\rangle_{L_3 R_3 L_1 R_1 L_2 R_2} &\longrightarrow \frac{1}{2}|00\rangle(|10\rangle + |01\rangle)(|10\rangle + |01\rangle) + \frac{1}{2}e^{i\theta_3}(|10\rangle - |01\rangle)(|10\rangle + |01\rangle)|00\rangle \\
&\quad + \frac{1}{\sqrt{2}}e^{i\theta_2}|00\rangle|00\rangle(|20\rangle - |02\rangle) + \frac{1}{2}e^{i(\theta_2+\theta_3)}(|10\rangle - |01\rangle)|00\rangle(|10\rangle - |01\rangle), \\
|\psi_{100}\rangle_{L_3 R_3 L_1 R_1 L_2 R_2} &\longrightarrow \frac{1}{\sqrt{2}}(|10\rangle + |01\rangle)|00\rangle|00\rangle + \frac{1}{\sqrt{2}}e^{i\theta_1}|00\rangle(|10\rangle - |01\rangle)|00\rangle, \\
|\psi_{010}\rangle_{L_3 R_3 L_1 R_1 L_2 R_2} &\longrightarrow \frac{1}{\sqrt{2}}|00\rangle(|10\rangle + |01\rangle)|00\rangle + \frac{1}{\sqrt{2}}e^{i\theta_2}|00\rangle|00\rangle(|10\rangle - |01\rangle), \\
|\psi_{001}\rangle_{L_3 R_3 L_1 R_1 L_2 R_2} &\longrightarrow \frac{1}{\sqrt{2}}|00\rangle|00\rangle(|10\rangle + |01\rangle) + \frac{1}{\sqrt{2}}e^{i\theta_3}(|10\rangle - |01\rangle)|00\rangle|00\rangle, \\
|\psi_{000}\rangle_{L_3 R_3 L_1 R_1 L_2 R_2} &\longrightarrow |00\rangle|00\rangle|00\rangle.
\end{aligned} \tag{28}$$

With the above equations, we can calculate the probability of a coincident click event:

$$\begin{aligned}
y^{R,R,R} &= (1-p_d)^3 \left[ \frac{3\eta^3 p_d}{16} + \frac{3\eta^2(1-\eta)}{4} \left( \frac{3}{4}p_d + \frac{1}{2}p_d^2 \right) + \frac{3\eta(1-\eta)^2}{2} p_d^2 + (1-\eta)^3 p_d^3 \right], \\
y^{L,L,L} &= (1-p_d)^3 \left[ \frac{\eta^3}{16} + \frac{3\eta^3 p_d}{16} + \frac{3\eta^2(1-\eta)}{4} \left( \frac{3}{4}p_d + \frac{1}{2}p_d^2 \right) + \frac{3\eta(1-\eta)^2}{2} p_d^2 + (1-\eta)^3 p_d^3 \right].
\end{aligned} \tag{29}$$

Finally, due to symmetry, we have

$$\begin{aligned}
y^{R,R,R} &= y^{R,L,L} = y^{L,R,L} = y^{L,L,R}, \\
y^{L,L,L} &= y^{R,R,L} = y^{R,L,R} = y^{L,R,R}.
\end{aligned} \tag{30}$$

### C. Four users with infinite decoy states

For the  $N = 4$  case, according from Eq. (12), the key rate formula is

$$R = \tilde{Y}_4^z [1 - H_2(\phi_4^z)] - \text{leak}_{\text{EC}}. \tag{31}$$

The number of joint three photon components in the  $\mathbf{Z}$ -basis is:

$$\begin{aligned} \tilde{Y}_4^z &= p_{\text{pair}} (p_\mu p_o \mu e^{-\mu} p_{\text{det}})^4 \sum_{a_1^e+a_1^l=1} \sum_{a_2^e+a_2^l=1} \sum_{a_3^e+a_3^l=1} \sum_{a_4^e+a_4^l=1} \left( \frac{y_{a_1^e a_1^l}^{P_4} y_{a_2^e a_2^l}^{P_1} y_{a_3^e a_3^l}^{P_2} y_{a_4^e a_4^l}^{P_3}}{q_{\text{tot}}^{P_1} q_{\text{tot}}^{P_2} q_{\text{tot}}^{P_3} q_{\text{tot}}^{P_4}} \right) \\ &= p_{\text{pair}} \frac{(p_\mu p_o \mu e^{-\mu} p_{\text{det}})^4}{q_{\text{tot}}^{P_1} q_{\text{tot}}^{P_2} q_{\text{tot}}^{P_3} q_{\text{tot}}^{P_4}} (2y_{10}y_{10}y_{10}y_{10} + 12y_{11}y_{10}y_{10}y_{00} + 2y_{11}y_{11}y_{00}y_{00}). \end{aligned} \quad (32)$$

When  $N = 4$ , there are  $2^4 = 16$  cases of intensity distribution in the  $\mathbf{Z}$ -basis. The probability of obtaining a joint three photon event in the  $\mathbf{X}$ -basis is calculated using the following relation:

$$\frac{\tilde{Y}_4^z}{\tilde{Y}_4^x} = \frac{\mu^4 e^{-4\mu} p_{[\mu, \mu, \mu, \mu]}}{(2\nu e^{-2\nu})^4 p_{[2\nu, 2\nu, 2\nu, 2\nu]}}, \quad (33)$$

where  $p_{[\mu, \mu, \mu, \mu]} = 16p_\mu p_o$ ,  $p_{[2\nu, 2\nu, 2\nu, 2\nu]} = \frac{2p_s^8}{M}$ . The four-party GHZ state  $|\Phi_0^+\rangle$  is used as the reference state:

$$\begin{aligned} |\Phi_0^+\rangle &= \frac{1}{\sqrt{2}} (|1111\rangle + |0000\rangle) \\ &= \frac{1}{\sqrt{2}} (|++++\rangle + |++--\rangle + |+-+-\rangle + |+--+\rangle + |-++-\rangle + |-+-+\rangle + |--++\rangle + |-- --\rangle) \end{aligned} \quad (34)$$

The probability of obtaining an error event of the joint three-photon components in the  $\mathbf{X}$ -basis is

$$\begin{aligned} e_4^x \tilde{Y}_4^x &= p_{\text{pair}} \left( \frac{2}{M} \right) \frac{(2\nu e^{-2\nu} p_\nu^2)^4}{q_{\text{tot}}^{P_1} q_{\text{tot}}^{P_2} q_{\text{tot}}^{P_3} q_{\text{tot}}^{P_4}} [(1 - e_d)(y^{R,L,L,L} + y^{L,R,L,L} + y^{L,L,R,L} + y^{L,L,L,R} + y^{R,R,R,L} + y^{R,R,L,R} \\ &\quad + y^{R,L,R,R} + y^{L,R,R,R}) + e_d(y^{L,L,L,L} + y^{L,L,R,R} + y^{L,R,L,R} + y^{L,R,R,L} + y^{R,L,L,R} + y^{R,L,R,L} \\ &\quad + y^{R,R,L,L} + y^{R,R,R,R})]. \end{aligned} \quad (35)$$

The input state is

$$\begin{aligned} &\frac{1}{\sqrt{2}} (|10\rangle_{a_1^e a_1^l} + e^{i\theta_1} |01\rangle_{a_1^e a_1^l}) \otimes \frac{1}{\sqrt{2}} (|10\rangle_{a_2^e a_2^l} + e^{i\theta_2} |01\rangle_{a_2^e a_2^l}) \otimes \frac{1}{\sqrt{2}} (|10\rangle_{a_3^e a_3^l} + e^{i\theta_3} |01\rangle_{a_3^e a_3^l}) \\ &\otimes \frac{1}{\sqrt{2}} (|10\rangle_{a_4^e a_4^l} + e^{i\theta_4} |01\rangle_{a_4^e a_4^l}) \end{aligned} \quad (36)$$

After passing through channel with transmittance  $\eta$  the state becomes a mixed state:

$$\begin{aligned} &\frac{\eta^4}{16} |\psi_{1111}\rangle \langle \psi_{1111}| + \frac{\eta^3(1-\eta)}{2} (|\psi_{1110}\rangle \langle \psi_{1110}| + |\psi_{1101}\rangle \langle \psi_{1101}| + |\psi_{1011}\rangle \langle \psi_{1011}| \\ &+ |\psi_{0111}\rangle \langle \psi_{0111}|) + \frac{3\eta^2(1-\eta)^2}{2} (|\psi_{1100}\rangle \langle \psi_{1100}| + |\psi_{1010}\rangle \langle \psi_{1010}| + |\psi_{1001}\rangle \langle \psi_{1001}| \\ &+ |\psi_{0110}\rangle \langle \psi_{0110}| + |\psi_{0101}\rangle \langle \psi_{0101}| + |\psi_{0011}\rangle \langle \psi_{0011}|) + 2\eta(1-\eta)^3 (|\psi_{1000}\rangle \langle \psi_{1000}| \\ &+ |\psi_{0100}\rangle \langle \psi_{0100}| + |\psi_{0010}\rangle \langle \psi_{0010}| + |\psi_{0001}\rangle \langle \psi_{0001}|) + (1-\eta)^4 |\psi_{0000}\rangle \langle \psi_{0000}| \end{aligned} \quad (37)$$

where

$$\begin{aligned} |\psi_{1111}\rangle_{a_1^e a_1^l a_2^e a_2^l a_3^e a_3^l a_4^e a_4^l} &= |10101010\rangle + e^{i\theta_4} |10101001\rangle + e^{i\theta_3} |10100110\rangle + e^{i(\theta_3+\theta_4)} |10100101\rangle \\ &+ e^{i\theta_2} |10011010\rangle + e^{i(\theta_2+\theta_4)} |10011001\rangle + e^{i(\theta_2+\theta_3)} |10010110\rangle + e^{i(\theta_2+\theta_3+\theta_4)} |10010101\rangle \\ &+ e^{i\theta_1} |01101010\rangle + e^{i(\theta_1+\theta_4)} |01101001\rangle + e^{i(\theta_1+\theta_3)} |01100110\rangle + e^{i(\theta_1+\theta_3+\theta_4)} |01100101\rangle \\ &+ e^{i(\theta_1+\theta_2)} |01011010\rangle + e^{i(\theta_1+\theta_2+\theta_3)} |01011001\rangle + e^{i(\theta_1+\theta_2+\theta_3)} |01010110\rangle \\ &+ e^{i(\theta_1+\theta_2+\theta_3+\theta_4)} |01010101\rangle, \end{aligned} \quad (38)$$

$$\begin{aligned}
|\psi_{1110}\rangle_{a_1^e a_1^l a_2^e a_2^l a_3^e a_3^l a_4^e a_4^l} &= |10101000\rangle + e^{i\theta_3}|10100100\rangle + e^{i\theta_2}|10011000\rangle + e^{i\theta_1}|01101000\rangle + e^{i(\theta_2+\theta_3)}|10010100\rangle \\
&\quad + e^{i(\theta_1+\theta_3)}|01100100\rangle + e^{i(\theta_1+\theta_2)}|01011000\rangle + e^{i(\theta_1+\theta_2+\theta_3)}|01010100\rangle, \\
|\psi_{1101}\rangle_{a_1^e a_1^l a_2^e a_2^l a_3^e a_3^l a_4^e a_4^l} &= |10100010\rangle + e^{i\theta_4}|10100001\rangle + e^{i\theta_2}|10010010\rangle + e^{i\theta_1}|01100010\rangle + e^{i(\theta_2+\theta_4)}|10010001\rangle \\
&\quad + e^{i(\theta_1+\theta_4)}|01100001\rangle + e^{i(\theta_1+\theta_2)}|01010010\rangle + e^{i(\theta_1+\theta_2+\theta_4)}|01010001\rangle, \\
|\psi_{1011}\rangle_{a_1^e a_1^l a_2^e a_2^l a_3^e a_3^l a_4^e a_4^l} &= |10001010\rangle + e^{i\theta_4}|10001001\rangle + e^{i\theta_3}|10000110\rangle + e^{i\theta_1}|01001010\rangle + e^{i(\theta_3+\theta_4)}|10000101\rangle \\
&\quad + e^{i(\theta_1+\theta_4)}|01001001\rangle + e^{i(\theta_1+\theta_3)}|01000110\rangle + e^{i(\theta_1+\theta_3+\theta_4)}|01000101\rangle, \\
|\psi_{0111}\rangle_{a_1^e a_1^l a_2^e a_2^l a_3^e a_3^l a_4^e a_4^l} &= |00101010\rangle + e^{i\theta_4}|00101001\rangle + e^{i\theta_3}|00100110\rangle + e^{i\theta_2}|00011010\rangle + e^{i(\theta_3+\theta_4)}|00100101\rangle \\
&\quad + e^{i(\theta_2+\theta_4)}|00011001\rangle + e^{i(\theta_2+\theta_3)}|00010110\rangle + e^{i(\theta_2+\theta_3+\theta_4)}|00010101\rangle, \\
|\psi_{1100}\rangle_{a_1^e a_1^l a_2^e a_2^l a_3^e a_3^l a_4^e a_4^l} &= |10100000\rangle + e^{i\theta_2}|10010000\rangle + e^{i\theta_1}|01100000\rangle + e^{i(\theta_1+\theta_2)}|01010000\rangle, \\
|\psi_{1010}\rangle_{a_1^e a_1^l a_2^e a_2^l a_3^e a_3^l a_4^e a_4^l} &= |10001000\rangle + e^{i\theta_3}|10000100\rangle + e^{i\theta_1}|01001000\rangle + e^{i(\theta_1+\theta_3)}|01000100\rangle, \\
|\psi_{1001}\rangle_{a_1^e a_1^l a_2^e a_2^l a_3^e a_3^l a_4^e a_4^l} &= |10000010\rangle + e^{i\theta_4}|10000001\rangle + e^{i\theta_1}|01000010\rangle + e^{i(\theta_1+\theta_4)}|01000001\rangle, \\
|\psi_{0110}\rangle_{a_1^e a_1^l a_2^e a_2^l a_3^e a_3^l a_4^e a_4^l} &= |00101000\rangle + e^{i\theta_3}|00100100\rangle + e^{i\theta_2}|00011000\rangle + e^{i(\theta_2+\theta_3)}|00010100\rangle, \\
|\psi_{0101}\rangle_{a_1^e a_1^l a_2^e a_2^l a_3^e a_3^l a_4^e a_4^l} &= |00100010\rangle + e^{i\theta_4}|00100001\rangle + e^{i\theta_2}|00010010\rangle + e^{i(\theta_2+\theta_4)}|00010001\rangle, \\
|\psi_{0011}\rangle_{a_1^e a_1^l a_2^e a_2^l a_3^e a_3^l a_4^e a_4^l} &= |00001010\rangle + e^{i\theta_4}|00001001\rangle + e^{i\theta_3}|00000110\rangle + e^{i(\theta_3+\theta_4)}|00000101\rangle, \\
|\psi_{1000}\rangle_{a_1^e a_1^l a_2^e a_2^l a_3^e a_3^l a_4^e a_4^l} &= |10000000\rangle + e^{i\theta_1}|01000000\rangle, \\
|\psi_{0100}\rangle_{a_1^e a_1^l a_2^e a_2^l a_3^e a_3^l a_4^e a_4^l} &= |00100000\rangle + e^{i\theta_2}|00010000\rangle, \\
|\psi_{0010}\rangle_{a_1^e a_1^l a_2^e a_2^l a_3^e a_3^l a_4^e a_4^l} &= |10000000\rangle + e^{i\theta_3}|01000000\rangle, \\
|\psi_{0001}\rangle_{a_1^e a_1^l a_2^e a_2^l a_3^e a_3^l a_4^e a_4^l} &= |10000000\rangle + e^{i\theta_4}|01000000\rangle, \\
|\psi_{0000}\rangle_{a_1^e a_1^l a_2^e a_2^l a_3^e a_3^l a_4^e a_4^l} &= |00000000\rangle.
\end{aligned} \tag{39}$$

Using the same method as the three-party scenario, consider that  $(\theta_1 + \theta_2 + \theta_3 + \theta_4)/\pi \pmod 2 = 0$ , we have the states before entering the detector. For simplicity, we skip the detailed procedures and give the result. The probability of a coincident click event is

$$\begin{aligned}
y_0^{R,L,L,L} &= p_4 \left( \frac{3}{2}p_d + \frac{1}{2}p_d^2 \right) + p_3 \left( \frac{1}{2}p_d + p_d^2 \right) + p_2' \left( \frac{3}{4}p_d^2 + \frac{1}{2}p_d^3 \right) + p_2'' p_d^2 + \frac{1}{2}p_1 p_d^3 + p_0 p_d^4, \\
y_0^{L,L,L,L} &= p_4 \left( \frac{1}{4} + \frac{3}{2}p_d + \frac{1}{2}p_d^2 \right) + p_3 \left( \frac{1}{2}p_d + p_d^2 \right) + p_2' \left( \frac{3}{4}p_d^2 + \frac{1}{2}p_d^3 \right) + p_2'' p_d^2 + \frac{1}{2}p_1 p_d^3 + p_0 p_d^4.
\end{aligned} \tag{40}$$

where

$$\begin{aligned}
p_4 &= \frac{\eta^4}{16}(1-p_d)^4, \quad p_3 = \frac{1}{2}\eta^3(1-\eta)(1-p_d)^4, \quad p_2' = \eta^2(1-\eta)^2(1-p_d)^4, \\
p_2'' &= \frac{1}{2}\eta^2(1-\eta)^2(1-p_d)^4, \quad p_1 = 2\eta(1-\eta)^3(1-p_d)^4, \quad p_0 = (1-\eta)^4(1-p_d)^4.
\end{aligned} \tag{41}$$

Because of the symmetric relation, we have the other terms

$$\begin{aligned}
y^{R,L,L,L} &= y^{L,R,L,L} = y^{L,L,R,L} = y^{L,L,L,R} = y^{R,R,R,L} = y^{R,R,L,R} = y^{R,L,R,R} = y^{L,R,R,R}, \\
y^{L,L,L,L} &= y^{L,L,R,R} = y^{L,R,L,R} = y^{L,R,R,L} = y^{R,L,L,R} = y^{R,L,R,L} = y^{R,R,L,L} = y^{R,R,R,R}.
\end{aligned} \tag{42}$$

#### D. Three users with three decoy states

Here we present the decoy formulas for the AMDI-QCKA protocol with three users and three decoy states. We consider the finite case. The secret key length  $l$  against coherent attacks in the finite-size regime can be given as

$$l \geq \underline{s}_0^z + \underline{s}_3^z [1 - H_2(\overline{\phi}_3^z)] - \text{leak}_{\text{EC}} - \log_2 \frac{4}{\varepsilon_{\text{cor}}} - 2 \log_2 \frac{2}{\epsilon' \hat{\epsilon}} - 2 \log_2 \frac{1}{2\varepsilon_{\text{PA}}}, \tag{43}$$

where we use  $\underline{x}$  ( $\bar{x}$ ) to denote the observed upper (lower) bound of  $x$ . We first briefly introduce the formulas of calculating the finite size effect. By using the Chernoff bound [39], given the expected value  $x^*$  and failure probability  $\epsilon$ , the upper bound and lower bound of the observed value can be given by  $\bar{x} = x^* + \frac{\beta}{2} + \sqrt{2\beta x^* + \frac{\beta^2}{4}}$ , and  $\underline{x} = x^* - \sqrt{2\beta x^*}$ , where  $\beta = \ln \epsilon^{-1}$ . Using the variant of Chernoff bound [39], we have the upper bound and lower bound of the expected value  $x^*$  for a given observed value  $x$  and failure probability  $\epsilon$ , which can be given as  $\bar{x}^* = x + \beta + \sqrt{2\beta x + \beta^2}$ , and  $\underline{x}^* = \max \left\{ x - \frac{\beta}{2} - \sqrt{2\beta x + \frac{\beta^2}{4}}, 0 \right\}$ . To obtain the upper bound of the phase error rate in the  $\mathbf{Z}$ -basis,  $\bar{\phi}_{11}^z$ , the random sampling theorem is utilized [39], which is given by  $\bar{\chi} \leq \lambda + \gamma^U(n, k, \lambda, \epsilon)$ , where  $\gamma^U(n, k, \lambda, \epsilon) = \left[ \frac{(1-2\lambda)AG}{n+k} + \sqrt{\frac{A^2G^2}{(n+k)^2} + 4\lambda(1-\lambda)G} \right] \left( 2 + 2\frac{A^2G}{(n+k)^2} \right)^{-1}$ , with  $A = \max\{n, k\}$  and  $G = \frac{n+k}{nk} \ln \frac{n+k}{2\pi nk\lambda(1-\lambda)\epsilon^2}$ .

By using the derivation method in Ref. [6], we have the lower bound of the number of joint three-photon states:

$$\begin{aligned} s_3^{z*} \geq & \frac{e^{-3\mu} p_{[\mu, \mu, \mu]}}{\nu^3 (\mu - \nu)} \left[ \mu^4 \left( e^{3\nu} \frac{n_{[\nu, \nu, \nu]}^*}{p_{[\nu, \nu, \nu]}} - e^{2\nu} \frac{\bar{n}_{[\nu, \nu, 0]}^*}{p_{[\nu, \nu, 0]}} - e^{2\nu} \frac{\bar{n}_{[\nu, 0, \nu]}^*}{p_{[\nu, 0, \nu]}} - e^{2\nu} \frac{\bar{n}_{[0, \nu, \nu]}^*}{p_{[0, \nu, \nu]}} + e^\nu \frac{n_{[\nu, 0, 0]}^*}{p_{[\nu, 0, 0]}} + e^\nu \frac{n_{[0, \nu, 0]}^*}{p_{[0, \nu, 0]}} \right. \right. \\ & + e^\nu \frac{n_{[0, 0, \nu]}^*}{p_{[0, 0, \nu]}} - \frac{\bar{n}_{[0, 0, 0]}^*}{p_{[0, 0, 0]}} \left. \right) - \nu^4 \left( e^{3\mu} \frac{\bar{n}_{[\mu, \mu, \mu]}^*}{p_{[\mu, \mu, \mu]}} - e^{2\mu} \frac{n_{[\mu, \mu, 0]}^*}{p_{[\mu, \mu, 0]}} - e^{2\mu} \frac{n_{[\mu, 0, \mu]}^*}{p_{[\mu, 0, \mu]}} - e^{2\mu} \frac{n_{[0, \mu, \mu]}^*}{p_{[0, \mu, \mu]}} \right. \\ & \left. \left. + e^\mu \frac{\bar{n}_{[\mu, 0, 0]}^*}{p_{[\mu, 0, 0]}} + e^\mu \frac{\bar{n}_{[0, \mu, 0]}^*}{p_{[0, \mu, 0]}} + e^\mu \frac{\bar{n}_{[0, 0, \mu]}^*}{p_{[0, 0, \mu]}} - \frac{n_{[0, 0, 0]}^*}{p_{[0, 0, 0]}} \right) \right]. \end{aligned} \quad (44)$$

For the data in the  $\mathbf{Z}$ -basis, we can also use  $[\mu, \mu, \nu]$ ,  $[\nu, \mu, \mu]$ ,  $[\mu, \nu, \mu]$ ,  $[\mu, \nu, \nu]$ ,  $[\nu, \mu, \nu]$ ,  $[\nu, \nu, \mu]$ ,  $[\nu, \nu, \nu]$  events to generate secret keys. In this case, we can replace term  $e^{-3\mu} p_{[\mu, \mu, \mu]}/\nu^3$  with  $p_{111}^z = (\mu^3 e^{-3\mu} p_{[\mu, \mu, \mu]} + 3\mu^2 \nu e^{-2\mu-\nu} p_{[\mu, \mu, \nu]} + 3\mu \nu^2 e^{-\mu-2\nu} p_{[\mu, \nu, \nu]} + \nu^3 e^{-3\nu} p_{[\mu, \mu, \mu]})/(\mu^3 \nu^3)$ .

The number of vacuum components, which is defined as the first user sends vacuum state, can be given by

$$s_0^{z*} = e^{-\mu} p_{[\mu, \mu, \mu]} \frac{n_{[0, \mu, \mu]}^*}{p_{[0, \mu, \mu]}} + 3e^{-\mu} p_{[\mu, \mu, \nu]} \frac{n_{[0, \mu, \nu]}^*}{p_{[0, \mu, \nu]}} + 3e^{-\mu} p_{[\mu, \nu, \nu]} \frac{n_{[0, \nu, \nu]}^*}{p_{[0, \nu, \nu]}} + e^{-\nu} p_{[\nu, \nu, \nu]} \frac{n_{[0, \nu, \nu]}^*}{p_{[0, \nu, \nu]}} \quad (45)$$

and  $s_3^{x*}$  can be calculated using following relation:

$$\frac{s_3^{z*}}{s_3^{x*}} = \frac{p_{111}^z}{(2\nu e^{-2\nu})^3 p_{[2\nu, 2\nu, 2\nu]}}. \quad (46)$$

The upper bound of joint three-photon errors of the  $\mathbf{X}$ -basis is

$$\begin{aligned} \bar{t}_3^x \leq & e^{-6\nu} p_{[2\nu, 2\nu, 2\nu]} \left( e^{6\nu} \frac{\bar{m}_{[2\nu, 2\nu, 2\nu]}^*}{p_{[2\nu, 2\nu, 2\nu]}} - e^{4\nu} \frac{n_{[2\nu, 2\nu, 0]}^*}{2p_{[2\nu, 2\nu, 0]}} - e^{4\nu} \frac{n_{[2\nu, 0, 2\nu]}^*}{2p_{[2\nu, 0, 2\nu]}} - e^{4\nu} \frac{n_{[0, 2\nu, 2\nu]}^*}{2p_{[0, 2\nu, 2\nu]}} \right. \\ & \left. + e^{2\nu} \frac{\bar{n}_{[2\nu, 0, 0]}^*}{2p_{[2\nu, 0, 0]}} + e^{2\nu} \frac{\bar{n}_{[0, 2\nu, 0]}^*}{2p_{[0, 2\nu, 0]}} + e^{2\nu} \frac{\bar{n}_{[0, 0, 2\nu]}^*}{2p_{[0, 0, 2\nu]}} - \frac{n_{[0, 0, 0]}^*}{2p_{[0, 0, 0]}} \right), \end{aligned} \quad (47)$$

where  $m_{[k_1^{\text{tot}}, k_2^{\text{tot}}, k_3^{\text{tot}}]}$  denotes the number of errors in the  $\mathbf{X}$ -basis of  $[k_1^{\text{tot}}, k_2^{\text{tot}}, k_3^{\text{tot}}]$  event. Using the random sampling theorem, with a failure probability  $\epsilon_e$ , the upper bound of single-photon pair phase error rate in the  $\mathbf{Z}$ -basis is

$$\bar{\phi}_3^z \leq \bar{e}_3^x + \gamma(s_3^z, s_3^x, \bar{e}_3^x, \epsilon_e), \quad (48)$$

where  $\bar{e}_3^x = \frac{\bar{t}_3^x}{s_3^x}$  is the upper bound of bit error rate in  $\mathbf{X}$ -basis.

## VI. SIMULATION FORMULAS

### A. Three party

In this section, we provide the simulation formulas for the AMDI-QCKA protocol. We begin with the three-user case. The user  $U_i$  send phase-randomized weak coherent pulse with random intensity  $k_i \in \{\mu_i, \nu_i, 0\}$ . When the

coherent state from  $U_1$ ,  $U_2$  and  $U_3$  arrive at the center relay and pass through the  $1 \times 2$  BS, the joint quantum states can be written as

$$|e^{i\theta_1} \sqrt{k_1 \eta_1}\rangle \otimes |e^{i\theta_2} \sqrt{k_2 \eta_2}\rangle \otimes |e^{i\theta_3} \sqrt{k_3 \eta_3}\rangle \xrightarrow{BS} |e^{i\theta_1} \sqrt{\frac{k_1 \eta_1}{2}}\rangle_{P_1} \otimes |e^{i\theta_3} \sqrt{\frac{k_3 \eta_3}{2}}\rangle_{P_1} \otimes |e^{i\theta_2} \sqrt{\frac{k_2 \eta_2}{2}}\rangle_{P_2} \otimes |e^{i\theta_1} \sqrt{\frac{k_1 \eta_1}{2}}\rangle_{P_2} \otimes |e^{i\theta_3} \sqrt{\frac{k_3 \eta_3}{2}}\rangle_{P_3} \otimes |e^{i\theta_2} \sqrt{\frac{k_2 \eta_2}{2}}\rangle_{P_3}, \quad (49)$$

where,  $\theta_i$  is the global phase of  $U_i$ ,  $\eta_i$  is the channel transmittance from  $U_i$  to the center relay,  $P_i$  represent the  $i$ -th detection port. After interfere at the BS, before entering the detector, the joint quantum state is

$$|e^{i\theta_1} \frac{\sqrt{k_1 \eta_1}}{2} + e^{i\theta_3} \frac{\sqrt{k_3 \eta_3}}{2}\rangle_{L_1} \otimes |e^{i\theta_1} \frac{\sqrt{k_1 \eta_1}}{2} - e^{i\theta_3} \frac{\sqrt{k_3 \eta_3}}{2}\rangle_{R_1} \otimes |e^{i\theta_2} \frac{\sqrt{k_2 \eta_2}}{2} + e^{i\theta_1} \frac{\sqrt{k_1 \eta_1}}{2}\rangle_{L_2} \otimes |e^{i\theta_2} \frac{\sqrt{k_2 \eta_2}}{2} - e^{i\theta_1} \frac{\sqrt{k_1 \eta_1}}{2}\rangle_{R_2} \otimes |e^{i\theta_3} \frac{\sqrt{k_3 \eta_3}}{2} + e^{i\theta_2} \frac{\sqrt{k_2 \eta_2}}{2}\rangle_{L_3} \otimes |e^{i\theta_3} \frac{\sqrt{k_3 \eta_3}}{2} - e^{i\theta_2} \frac{\sqrt{k_2 \eta_2}}{2}\rangle_{R_3}, \quad (50)$$

where  $L_i$  ( $R_i$ ) represents the left (right) side single-photon detector. Therefore, the probability of the detector  $L_i$  ( $R_i$ ) having a click can be given as

$$\begin{aligned} E_{L_1} &= 1 - (1 - p_d) \exp[-(\alpha_{13} + \beta_{13} \cos \theta_{13})], & E_{R_1} &= 1 - (1 - p_d) \exp[-(\alpha_{13} - \beta_{13} \cos \theta_{13})], \\ E_{L_2} &= 1 - (1 - p_d) \exp[-(\alpha_{21} + \beta_{21} \cos \theta_{21})], & E_{R_2} &= 1 - (1 - p_d) \exp[-(\alpha_{21} - \beta_{21} \cos \theta_{21})], \\ E_{L_3} &= 1 - (1 - p_d) \exp[-(\alpha_{32} + \beta_{32} \cos \theta_{32})], & E_{R_3} &= 1 - (1 - p_d) \exp[-(\alpha_{32} - \beta_{32} \cos \theta_{32})], \end{aligned} \quad (51)$$

where  $\alpha_{ij} = (k_i \eta_i + k_j \eta_j)/4$  ( $i, j \in \{1, 2, 3\}$ ),  $\beta_{ij} = \sqrt{k_i \eta_i k_j \eta_j}/2$ ,  $\theta_{ij} = \theta_i - \theta_j$ . Then, for each detector, we can calculate the probability of having a single click event. For example, for detector  $L_1$ , we have

$$\begin{aligned} q_{k_1 k_2 k_3}^{\theta_{13}, L_1} &= E_{L_1} (1 - E_{R_1}) (1 - E_{L_2}) (1 - E_{R_2}) (1 - E_{L_3}) (1 - E_{R_3}) \\ &= (1 - p_d)^5 e^{-[(\alpha_{13} + 2\alpha_{21} + 2\alpha_{32}) - \beta_{13} \cos \theta_{13}]} - (1 - p_d)^6 e^{-2(\alpha_{13} + \alpha_{21} + \alpha_{32})}. \end{aligned} \quad (52)$$

$q_{k_1 k_2 k_3}^{\theta_{13}, L_1}$  is the function of  $\theta_{13}$ , the phase difference between  $U_1$  and  $U_3$ . Through the same procedures, we have

$$\begin{aligned} q_{k_1 k_2 k_3}^{\theta_{13}, R_1} &= (1 - p_d)^5 e^{-[(\alpha_{13} + 2\alpha_{21} + 2\alpha_{32}) + \beta_{13} \cos \theta_{13}]} - (1 - p_d)^6 e^{-2(\alpha_{13} + \alpha_{21} + \alpha_{32})} \\ q_{k_1 k_2 k_3}^{\theta_{21}, L_2} &= (1 - p_d)^5 e^{-[(2\alpha_{13} + \alpha_{21} + 2\alpha_{32}) - \beta_{21} \cos \theta_{21}]} - (1 - p_d)^6 e^{-2(\alpha_{13} + \alpha_{21} + \alpha_{32})} \\ q_{k_1 k_2 k_3}^{\theta_{21}, R_2} &= (1 - p_d)^5 e^{-[(2\alpha_{13} + \alpha_{21} + 2\alpha_{32}) + \beta_{21} \cos \theta_{21}]} - (1 - p_d)^6 e^{-2(\alpha_{13} + \alpha_{21} + \alpha_{32})} \\ q_{k_1 k_2 k_3}^{\theta_{32}, L_3} &= (1 - p_d)^5 e^{-[(2\alpha_{13} + 2\alpha_{21} + \alpha_{32}) - \beta_{32} \cos \theta_{32}]} - (1 - p_d)^6 e^{-2(\alpha_{13} + \alpha_{21} + \alpha_{32})} \\ q_{k_1 k_2 k_3}^{\theta_{32}, R_3} &= (1 - p_d)^5 e^{-[(2\alpha_{13} + 2\alpha_{21} + \alpha_{32}) + \beta_{32} \cos \theta_{32}]} - (1 - p_d)^6 e^{-2(\alpha_{13} + \alpha_{21} + \alpha_{32})}. \end{aligned} \quad (53)$$

Therefore, the overall probability of having a single click is

$$\begin{aligned} q_{k_1 k_2 k_3} &= \left(\frac{1}{2\pi}\right)^3 \int_0^{2\pi} \int_0^{2\pi} \int_0^{2\pi} \left( q_{k_1 k_2 k_3}^{\theta_{13}, L_1} + q_{k_1 k_2 k_3}^{\theta_{13}, R_1} + q_{k_1 k_2 k_3}^{\theta_{21}, L_2} + q_{k_1 k_2 k_3}^{\theta_{21}, R_2} + q_{k_1 k_2 k_3}^{\theta_{32}, L_3} + q_{k_1 k_2 k_3}^{\theta_{32}, R_3} \right) d\theta_{13} d\theta_{21} d\theta_{32} \\ &= 2I_0(\beta_{13})(1 - p_d)^5 e^{-(\alpha_{13} + 2\alpha_{21} + 2\alpha_{32})} + 2I_0(\beta_{21})(1 - p_d)^5 e^{-(2\alpha_{13} + \alpha_{21} + 2\alpha_{32})} \\ &\quad + 2I_0(\beta_{32})(1 - p_d)^5 e^{-(2\alpha_{13} + 2\alpha_{21} + \alpha_{32})} - 6(1 - p_d)^6 e^{-2(\alpha_{13} + \alpha_{21} + \alpha_{32})}. \end{aligned} \quad (54)$$

To calculate the integration of  $\theta_{13}, \theta_{21}$  and  $\theta_{32}$ , we use the formulas for zero-order modified Bessel function of the first kind  $I_0(\sqrt{a^2 + b^2}x) = \frac{1}{2\pi} \int_0^{2\pi} e^{-x(a \cos \theta + b \sin \theta)} d\theta$ . The total probability of having a click event is  $q_{\text{tot}} = \sum_{k_1, k_2, k_3} q_{k_1 k_2 k_3}$ .

Separately calculate the integration, we have the probability that only detection port  $P_1$ ,  $P_2$  or  $P_3$  click

$$\begin{aligned} q_{k_1 k_2 k_3}^{P_1} &= 2I_0(\beta_{13})(1 - p_d)^5 e^{-(\alpha_{13} + 2\alpha_{21} + 2\alpha_{32})} - 2(1 - p_d)^6 e^{-2(\alpha_{13} + \alpha_{21} + \alpha_{32})}, \\ q_{k_1 k_2 k_3}^{P_2} &= 2I_0(\beta_{21})(1 - p_d)^5 e^{-(2\alpha_{13} + \alpha_{21} + 2\alpha_{32})} - 2(1 - p_d)^6 e^{-2(\alpha_{13} + \alpha_{21} + \alpha_{32})}, \\ q_{k_1 k_2 k_3}^{P_3} &= 2I_0(\beta_{32})(1 - p_d)^5 e^{-(2\alpha_{13} + 2\alpha_{21} + \alpha_{32})} - 2(1 - p_d)^6 e^{-2(\alpha_{13} + \alpha_{21} + \alpha_{32})}. \end{aligned} \quad (55)$$

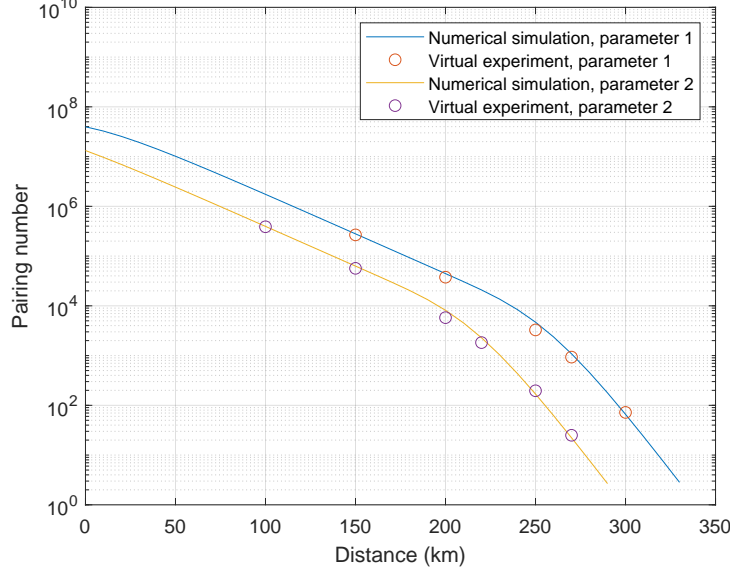


FIG. 7. Simulation result of the number of pairing event, where the circles represent  $n_{\text{tot}}$  obtained in virtual experiments, and the data points represent  $n_{\text{tot}}$  numerically calculated. We considered two set of parameters with different intensity. The comparison between our numerical formula and the virtual experiment results demonstrates a high level of agreement, indicating the accuracy of the numerical simulations.

The above probabilities are a function of the pulse intensity  $k_1, k_2, k_3$ . Take all the possible intensity combinations into account, we have the total probability of having a click at detection each port, which can be written as  $q_{\text{tot}}^{P_i} = \sum_{k_1, k_2, k_3} p_{k_1} p_{k_2} p_{k_3} q_{k_1 k_2 k_3}^{P_i}$ , where  $p_{k_i}$  is the probability of  $U_i$  choosing intensity  $k_i$ .

So far, we have finished the detection probability calculation of a single time bin. In the pairing step, detection events that occur in three different time bins at different detector ports are paired. Define the probability of obtaining a pairing event per pulse as  $p_{\text{pair}} := n_{\text{tot}}/\mathcal{N}$ , where  $n_{\text{tot}}$  is the number of pairing event. When the global phase of each user are locked, we have  $p_{\text{pair}} = \min\{q_{\text{tot}}^{P_1}, q_{\text{tot}}^{P_2}, q_{\text{tot}}^{P_3}\}$ , because almost all detection events can be paired. When the global phase locking is not utilized, the maximum pairing time interval between the earliest and the latest should be less than  $T_c$  to reduce the error rate. Given the earliest time bin with a click event (for example,  $P_1$ ), the probability of finding at least two click events in the other two different ports is  $(1 - (1 - q_{\text{tot}}^{P_2})^{\mathcal{N}T_c})(1 - (1 - q_{\text{tot}}^{P_3})^{\mathcal{N}T_c})$ , where  $\mathcal{N}T_c$  is the number of pulses that each user send within  $T_c$ . The average number of time bins that are required to obtain a pairing event is  $1 + 2/[1 - (1 - q_{\text{tot}}^{P_2})^{\mathcal{N}T_c}][1 - (1 - q_{\text{tot}}^{P_3})^{\mathcal{N}T_c}]$ . Then, by taking into account all possible detection ports, we have the probability of obtaining a pairing event for general  $N$  user case

$$p_{\text{pair}} = \sum_{i=1}^N q_{\text{tot}}^{P_i} \left\{ 1 + \frac{N-1}{\prod_{j=1, j \neq i}^N [1 - (1 - q_{\text{tot}}^{P_j})^{\mathcal{N}T_c}]} \right\}^{-1}. \quad (56)$$

To show the accuracy of Eq. (56), we perform a virtual experiment using computer, recorded  $n_{\text{tot}}$  and compared with that computed using the above formula. As shown in Fig. 7, the result of Eq. (56) fit well with the virtual experiment. In simulation, we assume the mean pairing time interval (the maximum time interval between the first and the last time bin) is  $T_{\text{mean}} = T_c/2$ .

Then, we consider the number of the paired event with intensities  $[k_1^{\text{tot}}, k_2^{\text{tot}}, k_3^{\text{tot}}]$  (except  $[2\nu_1, 2\nu_2, 2\nu_3]$ ), which is

$$n_{[k_1^{\text{tot}}, k_2^{\text{tot}}, k_3^{\text{tot}}]} = n_{\text{tot}} \sum_{k_1^e + k_1^l = k_1^{\text{tot}}} \sum_{k_2^e + k_2^l = k_2^{\text{tot}}} \sum_{k_3^e + k_3^l = k_3^{\text{tot}}} \left( \frac{p_{k_1^e} p_{k_3^l} q_{k_1^e k_3^l}^{P_1}}{q_{\text{tot}}^{P_1}} \frac{p_{k_1^l} p_{k_2^e} q_{k_2^e k_1^l}^{P_2}}{q_{\text{tot}}^{P_2}} \frac{p_{k_2^l} p_{k_3^e} q_{k_3^e k_2^l}^{P_3}}{q_{\text{tot}}^{P_3}} \right). \quad (57)$$

In calculating the pairing event  $n_{[k_1^{\text{tot}}, k_2^{\text{tot}}, k_3^{\text{tot}}]}$ , the click event of each port is mainly relevant to the intensity and phase of two neighbor users. Take  $P_1$  as an example, the pairing event  $n_{[2\nu_1, 2\nu_2, 2\nu_3]}$  requires  $U_1(U_3)$  sends  $\nu_1(\nu_3)$  at the

time bin when  $P_1$  clicks, while Bob may choose any intensities including  $\mu_2$ ,  $\nu_2$  and 0. The probability of having a click at  $P_1$  is the function of intensities  $k_1$ ,  $k_2$ ,  $k_3$ . In calculation, for simplification we should first sum all Bob's possible intensities. The probability of having a click event in each detection port is given as  $q_{k_1^e k_3^l}^{P_1} = \sum_{k_2} p_{k_2} q_{k_1^e k_2 k_3^l}^{P_1}$ ,

$$q_{k_2^e k_1^l}^{P_2} = \sum_{k_3} p_{k_3} q_{k_1^l k_2^e k_3}^{P_2}, \text{ and } q_{k_3^e k_2^l}^{P_3} = \sum_{k_1} p_{k_1} q_{k_1 k_2^l k_3^e}^{P_3}.$$

For simplicity, in the following we consider the symmetric case. All the users choose the same intensity set,  $\mu_1 = \mu_2 = \dots = \mu_N = \mu$  and  $\nu_1 = \nu_2 = \dots = \nu_N = \nu$ . We take  $U_1$  as the reference and assume marginal bit error rate between each users are equal in symmetric case. The maximum  $\mathbf{Z}$ -basis marginal bit error can be written as  $E_{1,2}^z = m_{1,2}^z/n_{[\mu,\mu,\mu]}$ , the error rate between  $U_1$  and  $U_2$ . There are four terms contribute to error rate between  $U_1$  and  $U_2$ :

$$m_{1,2}^z = n_{\text{tot}} \frac{(p_\mu p_\nu)^3}{q_{\text{tot}}^{P_1} q_{\text{tot}}^{P_2} q_{\text{tot}}^{P_3}} \left( q_{\mu 0}^{P_1} q_{00}^{P_2} q_{\mu\mu}^{P_3} + q_{\mu\mu}^{P_1} q_{00}^{P_2} q_{0\mu}^{P_3} + q_{00}^{P_1} q_{\mu\mu}^{P_2} q_{\mu 0}^{P_3} + q_{00}^{P_1} q_{\mu\mu}^{P_2} q_{00}^{P_3} \right) \quad (58)$$

The number of  $\mathbf{X}$ -basis event,  $n_{[2\nu,2\nu,2\nu]}$ , can be given as

$$n_{[2\nu,2\nu,2\nu]} = \frac{n_{\text{tot}} p_\nu^6}{2M\pi^2} \int_0^{2\pi} \int_0^{2\pi} \left( \frac{q_{\nu\nu}^{\theta_{13},P_1}}{q_{\text{tot}}^{P_1}} \frac{q_{\nu\nu}^{\theta_{21},P_2}}{q_{\text{tot}}^{P_2}} \frac{q_{\nu\nu}^{-(\theta_{13}+\theta_{21}),P_3}}{q_{\text{tot}}^{P_3}} \right) d\theta_{13} d\theta_{21}. \quad (59)$$

where  $q_{\nu\nu}^{\theta_{13},P_1} = \sum_{k_2} p_{k_2} (q_{\nu k_2\nu}^{\theta_{13},L_1} + q_{\nu k_2\nu}^{\theta_{13},R_1})$ ,  $q_{\nu\nu}^{\theta_{21},P_2} = \sum_{k_3} p_{k_3} (q_{\nu\nu k_3}^{\theta_{21},L_2} + q_{\nu\nu k_3}^{\theta_{21},R_2})$ ,  $q_{\nu\nu}^{\theta_{32},P_3} = \sum_{k_1} p_{k_1} (q_{\theta_{32},L_3} + q_{\theta_{32},R_3})$ . The global phase of each user arriving at Eve is continuous and random due to phase drift in the fibre. The phase matching condition of the  $\mathbf{X}$ -basis paired event is  $(\theta_{13} + \theta_{21} + \theta_{32}) \bmod \pi = 1$  or 0. The total number of errors in the  $\mathbf{X}$ -basis can be written as

$$m_{[2\nu,2\nu,2\nu]} = \frac{n_{\text{tot}} p_\nu^6}{2M\pi^2 q_{\text{tot}}^{P_1} q_{\text{tot}}^{P_2} q_{\text{tot}}^{P_3}} \int_0^{2\pi} \int_0^{2\pi} \left[ (1 - e_d) \left( y_{6\nu}^{R,R,R} + y_{6\nu}^{R,L,L} + y_{6\nu}^{L,R,L} + y_{6\nu}^{L,L,R} \right) \right. \\ \left. + e_d \left( y_{6\nu}^{L,L,L} + y_{6\nu}^{L,R,R} + y_{6\nu}^{R,L,R} + y_{6\nu}^{R,R,L} \right) \right] d\theta_{13} d\theta_{21}, \quad (60)$$

where  $y_{6\nu}^{R(L),R(L),R(L)} = \frac{\theta_{13},R_1(L_1)}{q_{\nu\nu}} \frac{\theta_{21},R_1(L_1)}{q_{\nu\nu}} \frac{\theta_{32}+\delta,R_1(L_1)}{q_{\nu\nu}}$ ,  $y_{6\nu}^{\theta_{13},L_1(R_1)} = \sum_{k_2} p_{k_2} q_{\nu k_2\nu}^{\theta_{13},L_1(R_1)}$ ,  $y_{6\nu}^{\theta_{21},L_2(R_2)} = \sum_{k_3} p_{k_3} q_{\nu\nu k_3}^{\theta_{21},L_2(R_2)}$ ,  $y_{6\nu}^{\theta_{32},L_3(R_3)} = \sum_{k_1} p_{k_1} q_{k_1\nu\nu}^{\theta_{32},L_3(R_3)}$ ,  $\delta = T_{\text{mean}}(2\pi\Delta f + \omega_{\text{fiber}}) + \frac{\pi}{M}$  is the phase misalignment,  $\Delta f$  is the laser frequency difference,  $\omega_{\text{fiber}}$  is fiber phase drift rate, and  $\frac{\pi}{M}$  is the result of finite phase slice width.

The intrinsic interference error rate for three-party is approximately 37.5%. Let  $s_{u_1 u_2 u_3}$  represents there are  $u_i$  ( $i = 1, 2, 3$ ) photons from  $U_i$ . The bit error rate in the  $\mathbf{X}$ -basis can be written as  $E_X \approx \frac{6e_0 s_{210}}{s_{111} + 6s_{210}} = 37.5\%$ , where  $e_0 = 0.5$  is the vacuum state error rate.

## B. Four party

In this section, we briefly introduce the simulation formulas for the AMDI-QCKA protocol with four party. For simplicity, we omit the detailed state evolution. Given the four users send intensity  $k_1$ ,  $k_2$ ,  $k_3$  and  $k_4$ , the overall probability of having a single click is

$$q_{k_1 k_2 k_3 k_4} = 2I_0(\beta_{14})(1 - p_d)^7 e^{-(\alpha_{14} + 2\alpha_{21} + 2\alpha_{32} + 2\alpha_{43})} + 2I_0(\beta_{21})(1 - p_d)^7 e^{-(2\alpha_{14} + \alpha_{21} + 2\alpha_{32} + 2\alpha_{43})} \\ + 2I_0(\beta_{32})(1 - p_d)^7 e^{-(2\alpha_{14} + 2\alpha_{21} + \alpha_{32} + 2\alpha_{43})} + 2I_0(\beta_{43})(1 - p_d)^7 e^{-(2\alpha_{14} + 2\alpha_{21} + 2\alpha_{32} + \alpha_{43})} \\ - 8(1 - p_d)^8 e^{-2(\alpha_{14} + \alpha_{21} + \alpha_{32} + \alpha_{43})}. \quad (61)$$

We also have the probability that only port 1, 2, 3 or 4 click

$$q_{k_1, k_2, k_3, k_4}^{P_1} = 2I_0(\beta_{14})(1 - p_d)^7 e^{-(\alpha_{14} + 2\alpha_{21} + 2\alpha_{32} + 2\alpha_{43})} - 2(1 - p_d)^8 e^{-2(\alpha_{14} + \alpha_{21} + \alpha_{32} + \alpha_{43})}, \\ q_{k_1, k_2, k_3, k_4}^{P_2} = 2I_0(\beta_{21})(1 - p_d)^7 e^{-(2\alpha_{14} + \alpha_{21} + 2\alpha_{32} + 2\alpha_{43})} - 2(1 - p_d)^8 e^{-2(\alpha_{14} + \alpha_{21} + \alpha_{32} + \alpha_{43})}, \\ q_{k_1, k_2, k_3, k_4}^{P_3} = 2I_0(\beta_{32})(1 - p_d)^7 e^{-(2\alpha_{14} + 2\alpha_{21} + \alpha_{32} + 2\alpha_{43})} - 2(1 - p_d)^8 e^{-2(\alpha_{14} + \alpha_{21} + \alpha_{32} + \alpha_{43})}, \\ q_{k_1, k_2, k_3, k_4}^{P_4} = 2I_0(\beta_{43})(1 - p_d)^7 e^{-(2\alpha_{14} + 2\alpha_{21} + 2\alpha_{32} + \alpha_{43})} - 2(1 - p_d)^8 e^{-2(\alpha_{14} + \alpha_{21} + \alpha_{32} + \alpha_{43})}. \quad (62)$$

The total number of  $[k_1^{\text{tot}}, k_2^{\text{tot}}, k_3^{\text{tot}}, k_4^{\text{tot}}]$  event (except  $[2\nu, 2\nu, 2\nu, 2\nu]$  event) is

$$n_{[k_1^{\text{tot}}, k_2^{\text{tot}}, k_3^{\text{tot}}, k_4^{\text{tot}}]} = n_{\text{tot}} \sum_{i=1, k_i^e + k_i^l = k_i^{\text{tot}}}^N \left( \frac{p_{k_1^e} p_{k_4^l} q_{k_1^e k_4^l}^{P_1}}{q_{\text{tot}}^{P_1}} \frac{p_{k_2^e} p_{k_1^l} q_{k_2^e k_1^l}^{P_2}}{q_{\text{tot}}^{P_2}} \frac{p_{k_3^e} p_{k_2^l} q_{k_3^e k_2^l}^{P_3}}{q_{\text{tot}}^{P_3}} \frac{p_{k_4^e} p_{k_3^l} q_{k_4^e k_3^l}^{P_4}}{q_{\text{tot}}^{P_4}} \right), \quad (63)$$

where  $q_{\text{tot}}^{P_i} = \sum_{k_1, k_2, k_3, k_4} p_{k_1} p_{k_2} p_{k_3} p_{k_4} q_{k_1 k_2 k_3 k_4}^{P_i}$ . Assume the maximum marginal error rate is the error rate between  $U_1$  and  $U_2$ . There are eight terms contribute to error rate between  $U_1$  and  $U_2$ :

$$m_{1,2}^z = n_{\text{tot}} \frac{(p_\mu p_o)^4}{q_{\text{tot}}^{P_1} q_{\text{tot}}^{P_2} q_{\text{tot}}^{P_3} q_{\text{tot}}^{P_4}} \left( q_{\mu 0}^{P_1} q_{00}^{P_2} q_{\mu\mu}^{P_3} q_{0\mu}^{P_4} + q_{\mu\mu}^{P_1} q_{00}^{P_2} q_{\mu\mu}^{P_3} q_{00}^{P_4} + q_{\mu 0}^{P_1} q_{00}^{P_2} q_{\mu 0}^{P_3} q_{\mu\mu}^{P_4} + q_{\mu\mu}^{P_1} q_{00}^{P_2} q_{\mu 0}^{P_3} q_{\mu 0}^{P_4} \right. \\ \left. + q_{00}^{P_1} q_{\mu\mu}^{P_2} q_{0\mu}^{P_3} q_{0\mu}^{P_4} + q_{0\mu}^{P_1} q_{\mu\mu}^{P_2} q_{0\mu}^{P_3} q_{00}^{P_4} + q_{00}^{P_1} q_{\mu\mu}^{P_2} q_{00}^{P_3} q_{\mu\mu}^{P_4} + q_{0\mu}^{P_1} q_{\mu\mu}^{P_2} q_{00}^{P_3} q_{\mu 0}^{P_4} \right) \quad (64)$$

The number of  $[2\nu, 2\nu, 2\nu, 2\nu]$  event is

$$n_{[2\nu, 2\nu, 2\nu, 2\nu]} = \frac{n_{\text{tot}} p_\nu^8}{4M\pi^3} \int_0^{2\pi} \int_0^{2\pi} \int_0^{2\pi} \left( \frac{q_{\nu\nu}^{\theta_{14}, P_1}}{q_{\text{tot}}^{P_1}} \frac{q_{\nu\nu}^{\theta_{21}, P_2}}{q_{\text{tot}}^{P_2}} \frac{q_{\nu\nu}^{\theta_{32}, P_3}}{q_{\text{tot}}^{P_3}} \frac{q_{\nu\nu}^{-(\theta_{14} + \theta_{21} + \theta_{32}), P_4}}{q_{\text{tot}}^{P_4}} \right) d\theta_{14} d\theta_{21} d\theta_{32}, \quad (65)$$

where  $q_{\nu\nu}^{\theta, P_i}$  can be calculated with the same method as the three-user case. The total number of errors in the  $\mathbf{X}$ -basis can be given as

$$m_{[2\nu, 2\nu, 2\nu, 2\nu]} = \frac{n_{\text{tot}} p_\nu^8}{4M\pi^3 q_{\text{tot}}^{P_1} q_{\text{tot}}^{P_2} q_{\text{tot}}^{P_3} q_{\text{tot}}^{P_4}} \int_0^{2\pi} \int_0^{2\pi} \int_0^{2\pi} \left[ (1 - e_d) \left( y_{8\nu}^{R, L, L, L} + y_{8\nu}^{L, R, L, L} + y_{8\nu}^{L, L, R, L} + y_{8\nu}^{L, L, L, R} \right. \right. \\ \left. \left. + y_{8\nu}^{R, R, R, L} + y_{8\nu}^{R, R, L, R} + y_{8\nu}^{R, L, R, R} + y_{8\nu}^{L, R, R, R} \right) + e_d \left( y_{8\nu}^{L, L, L, L} + y_{8\nu}^{L, L, R, R} + y_{8\nu}^{L, R, L, R} + y_{8\nu}^{L, R, R, L} \right. \right. \\ \left. \left. + y_{8\nu}^{R, L, L, R} + y_{8\nu}^{R, L, R, L} + y_{8\nu}^{R, R, L, L} + y_{8\nu}^{R, R, R, R} \right) \right] d\theta_{14} d\theta_{21} d\theta_{32}. \quad (66)$$

where  $y_{8\nu}^{R(L), R(L), R(L), R(L)} = \frac{\theta_{14}, R_1(L_1)}{q_{\nu\nu}} \frac{\theta_{21} + \delta, R_2(L_2)}{q_{\nu\nu}} \frac{\theta_{32} + \delta, R_3(L_3)}{q_{\nu\nu}} \frac{\theta_{43} + \delta, R_4(L_4)}{q_{\nu\nu}}$ , and  $q_{\nu\nu}^{\theta, R_i(L_i)}$  can be obtained by using the same method as the three-user case.

The intrinsic interference error rate for four-party case in the  $\mathbf{X}$ -basis can be approximately written as  $E_X \approx \frac{12e_0 s_{2110}}{s_{1111} + 12s_{2110}} \approx 42.86\%$ .